

Inter- and Intramolecular Hydrogen-Bonding Interaction of Hydroxo Groups and Steric Effect of Alkyl Substituents on Pyrazolyl Rings in Tp^{R} Ligands: Synthesis and Structural Characterization of Chloro-, Acetylacetonato-, and Hydroxo Complexes of VO^{2+} with $\text{Tp}^{\text{Pr}^i_2}$ and Tp^{Me_2} Ligands[†]

Masahiro Kosugi, Shiro Hikichi,* Munetaka Akita, and Yoshihiko Moro-oka*

Research Laboratory of Resources Utilization, Tokyo Institute of Technology, 4259 Nagatsuta, Midori-ku, Yokohama 226-8503, Japan

Received May 29, 1998

Novel vanadyl (VO^{2+}) chloro and hydroxo complexes with the hindered $\text{Tp}^{\text{Pr}^i_2}$ (hydrotris(3,5-diisopropyl-1-pyrazolyl)borate) and Tp^{Me_2} (hydrotris(3,5-dimethylpyrazolyl-1-pyrazolyl)borate) ligands were prepared and structurally characterized successfully. Ligand displacement of $\text{VOCl}_2(\text{MeCN})_2(\text{H}_2\text{O})$ by Tp^{R} afforded a series of octahedral chloro complexes, $\text{Tp}^{\text{R}}\text{V}(\text{O})(\text{Cl})(\text{X})$ (**1**: $\text{R} = \text{Pr}^i_2$, $\text{X} = \text{Pz}^{\text{Pr}^i_2}\text{H}$; **2**: $\text{R} = \text{Pr}^i_2$, $\text{X} = \text{py}$; **6**: $\text{R} = \text{Me}_2$, $\text{X} = \text{NCMe}$). Hydrolysis of the obtained chloro complexes yielded the corresponding hydroxo complexes **4**, **5**, and **7**, but their structures were very unique and different from that of the previously reported dinuclear VO^{2+} bis(μ -hydroxo) complex with the less hindered Tp^{H_2} (hydrotris(1-pyrazolyl)borate) ligand. For the $\text{Tp}^{\text{Pr}^i_2}$ complexes, the octahedral hydroxo-aqua complex, $\text{Tp}^{\text{Pr}^i_2}\text{V}(\text{O})(\text{OH})(\text{OH}_2)$ (**4**), and the trinuclear bis(μ -hydroxo)bis(μ -pyrazolato) complex, $\text{Tp}^{\text{Pr}^i_2}\text{V}(\text{O})(\mu\text{-OH})(\mu\text{-Pz}^{\text{Pr}^i_2})\text{V}(\text{O})(\mu\text{-OH})(\mu\text{-Pz}^{\text{Pr}^i_2})\text{V}(\text{O})\text{Tp}^{\text{Pr}^i_2}$ (**5**), were isolated. The hydroxo-aqua complex **4** was dimerized through the intermolecular hydrogen-bonding interaction between the hydroxo and aqua ligands forming the H_3O_2^- bridging ligand. The trinuclear complex **5** consisted of two octahedral $\text{Tp}^{\text{Pr}^i_2}\text{V}(\text{O})$ fragments and a distorted trigonal-bipyramidal non- $\text{Tp}^{\text{Pr}^i_2}$ -supported VO^{2+} center, sitting on the pseudo C_2 symmetry axis, and was formed via coupling of **4** and the VO^{2+} -pyrazolato species, resulting from partial decomposition of the chloro complexes during the hydrolysis. Steric repulsion of the bulky Pr^i groups in $\text{Tp}^{\text{Pr}^i_2}$ might hinder the formation of a dinuclear bis(μ -hydroxo) complex like the Tp^{H_2} and Tp^{Me_2} derivatives. The dinuclear bis(μ -hydroxo) complex with the Tp^{Me_2} ligand, $(\kappa^3\text{-Tp}^{\text{Me}_2})\text{V}(\text{O})(\mu\text{-OH})_2\text{V}(\text{O})(\kappa^2\text{-Tp}^{\text{Me}_2})$ (**7**), consisted of *syn*-arranged $\text{V}=\text{O}$ fragments, having the different coordination geometries of the vanadium centers (octahedron with $\kappa^3\text{-Tp}^{\text{Me}_2}$ and trigonal bipyramid with $\kappa^2\text{-Tp}^{\text{Me}_2}$). Intramolecular hydrogen-bonding interaction between one of the two hydroxo groups and the noncoordinated pyrazolyl nitrogen atom in $\kappa^2\text{-Tp}^{\text{Me}_2}$ was observed.

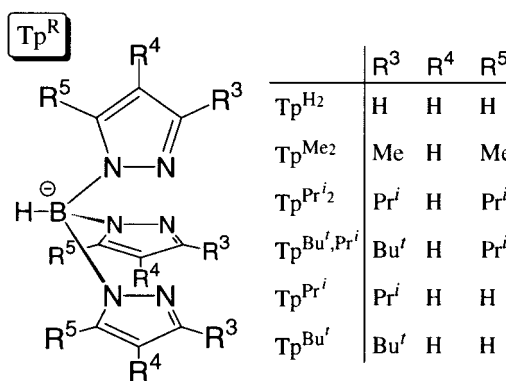
Introduction

During last three decades, a family of tris(pyrazolyl)borates has been widely used as supporting ligands for various inorganic and organometallic compounds.¹ One of the advantages of the tris(pyrazolyl)borate ligands is the ease of controlling the properties of metal complexes (coordination environment and reactivity of metal centers, solubility in organic solvents, facility of crystallization, etc.) by introduction of various substituents onto the pyrazolyl rings. It is notable that highly sterically demanding hydrotris(pyrazolyl)borate ligands, containing bulky substituents at the 3- and 5-positions of pyrazole rings (Tp^{R} , see Chart 1), can control coordination environments of the metal centers and prevent formation of coordinatively saturated less reactive complexes ($\text{Tp}^{\text{R}_2}\text{M}$), which are similar to the “full-sandwich-type” cyclopentadienyl (Cp) ligand complexes (Cp_2M).

[†] Abbreviations used in this paper: Tp^{R} , hydrotris(3,5-substituted-1-pyrazolyl)borate; Tp^{H_2} , hydrotris(1-pyrazolyl)borate; Tp^{Me_2} , hydrotris(3,5-dimethyl-1-pyrazolyl)borate; $\text{Tp}^{\text{Pr}^i_2}$, hydrotris(3,5-diisopropyl-1-pyrazolyl)borate; $\text{Tp}^{\text{Bu}^i, \text{Pr}^i}$, hydrotris(3-*tert*-butyl-5-isopropyl-1-pyrazolyl)borate; Tp^{Pr^i} , hydrotris(3-isopropyl-1-pyrazolyl)borate; Tp^{Bu^i} , hydrotris(3-*tert*-butyl-1-pyrazolyl)borate; $\text{Pz}^{\text{Me}_2}\text{H}$, 3,5-dimethylpyrazole; $\text{Pz}^{\text{Pr}^i}\text{H}$, 3,5-diisopropylpyrazole; DMF, dimethylformamide; py, pyridine; acac, acetylacetonato.

(1) (a) Trofimenko, S. *Chem. Rev.* **1993**, *93*, 943. (b) Kitajima, N.; Tolman, W. B. *Prog. Inorg. Chem.* **1995**, *43*, 419. (c) Parkin, G. *Adv. Inorg. Chem.* **1995**, *42*, 291. (d) Reger, D. L. *Coord. Chem. Rev.* **1996**, *147*, 571.

Chart 1



In our laboratory, dioxygen complexes of Mn, Fe, and Cu with the sterically hindered hydrotris(3,5-diisopropyl-1-pyrazolyl)borate ($\text{Tp}^{\text{Pr}^i_2}$) have been investigated from the bioinorganic standpoint.^{1b} Especially, a series of hydroxo complexes of divalent metals are found to be versatile starting materials for various complexes due to their capability of dehydrative condensation with protic substrates, including XOOH ($\text{X} = \text{H}$, alkyl, acyl), as found for the formation of $\mu\text{-}\eta^2\text{:}\eta^2\text{-peroxo}$, alkylperoxo, and acylperoxo complexes of $\text{Cu}(\text{II})$.^{1b,2} In addition, the dinuclear $\text{Mn}(\text{II})$ bis(μ -hydroxo) complex shows O_2 activa-

tion capability, although other Mn(II) complexes with carboxylate or halide ligands do not react with O₂; in the oxygenation reaction of the Mn(II)–OH complex, the hydroxo ligand is oxidized to an oxo ligand and/or serves as a good leaving group (eliminates as H₂O).³ Recently, we are extending our synthetic targets to dioxigen complexes of various metal ions, ranging from the biologically irrelevant late transition metals⁴ (Co, Ni, Ru, Rh, Pd; i.e., they do not participate in O₂ metabolism, although Co and Ni are essential for life) to the early transition metals. Systematic investigations of various metal complexes having the same Tp^R ligand may provide us insight into the role of the metal ions and the effect of the supporting ligands in various oxidation reactions.

Because vanadium–dioxigen species are known to take part in various chemical and biological oxidation processes,^{5–7} chemistry of Tp^{Pr₂V}–dioxigen complexes is extremely attractive. Several vanadium complexes with the less hindered Tp^R (R = H₂ or Me₂) ligands have been reported previously.^{8–12} However, no example of structurally characterized highly hindered Tp^R (R = bulkier than Me) complexes of vanadium

is known so far. Herein, we report the synthesis and structural characterization of chloro- and hydroxovanadium(IV) complexes with the hindered Tp^{Pr₂} ligand. As indicated above, hydroxo complexes are expected to be useful starting compounds for novel complexes by dehydrative condensation or oxidation. Thus, synthesis of a V(IV)–hydroxo complex with Tp^{Pr₂} is the first subject of our study on vanadium chemistry. In this study, Tp^{Me₂} derivatives are also prepared in order to reveal the steric effect of the Tp^R substituents on structures of coordination environments of the vanadyl (VO²⁺) centers, and discussion is focused on the synthesis and structural characterization of the novel Tp^RV^{IV}(O) complexes.

Experimental Section

Instrumentation. IR measurements were carried out as KBr pellets or CH₂Cl₂ solutions, using a JASCO FT/IR-5300 spectrometer. Field desorption mass spectra were recorded on a Hitachi M-80 mass spectrometer. UV–vis spectra were recorded on Shimadzu UV-260 or JASCO V-570 spectrometers. ESR and ¹H NMR spectra were recorded on JEOL RE-3X and Bruker AC-200 spectrometers, respectively.

Materials and Methods. All solvents used were purified by the literature methods.¹³ The aqueous NaOH solution was degassed with argon bubbling for 60 min prior to use. The reagents of the highest grade commercially available were used without further purification. All manipulations were performed under argon by standard Schlenk techniques. VOCl₂(MeCN)₂(H₂O),¹⁴ KTp^{Pr₂},^{2b} and KTp^{Bu_tPr_i}¹⁵ were prepared by the methods reported previously. NaTp^{Me₂} and NaTp^{Pr₂} were prepared by the reaction of the corresponding pyrazoles and NaBH₄ with the similar manner for the preparation of KTp^R.

Tp^{Pr₂}V(O)(Cl)(Pz^{Pr₂}H) (1). KTp^{Pr₂} (5.7 × 10³ mg; 11 mmol) was added to a MeCN solution (150 mL) of VOCl₂(MeCN)₂(H₂O) (2.6 × 10³ mg; 11 mmol), and this reaction mixture was stirred for 1 h at 50 °C. After removal of the solvent under vacuum, the resulting solid was extracted with pentane. Concentration of the blue pentane extract followed by refrigeration at –20 °C afforded blue precipitates, which were collected by filtration. Then, the resulting blue solid of **1** was washed with a minimal amount of pentane and dried under vacuum (4.3 × 10³ mg; 5.9 mmol; 54% yield). Anal. Calcd for C₃₆H₆₂N₈OBClV: C, 60.04; H, 8.68; N, 15.56; Cl, 4.92. Found: C, 59.49; H, 8.57; N, 15.25; Cl, 4.61. IR (KBr pellet, ν/cm⁻¹): 3431 (pyrazole NH), 2544 (BH), 1561 (pyrazole C=N), 1537 (Tp^{Pr₂}-pyrazolyl C=N), 977

- (2) (a) Kitajima, N.; Hikichi, S.; Tanaka, M.; Moro-oka, Y. *J. Am. Chem. Soc.* **1993**, *115*, 5496. (b) Kitajima, N.; Fujisawa, K.; Fujimoto, C.; Moro-oka, Y.; Hashimoto, S.; Kitagawa, T.; Toriumi, K.; Tatsumi, K.; Nakamura, A. *J. Am. Chem. Soc.* **1992**, *114*, 1277. (c) Kitajima, N.; Tamura, N.; Tanaka, M.; Moro-oka, Y. *Inorg. Chem.* **1992**, *31*, 6402. (d) Kitajima, N.; Singh, U. P.; Amagai, H.; Osawa, M.; Moro-oka, Y. *J. Am. Chem. Soc.* **1991**, *113*, 7757. (e) Hikichi, S.; Ogiwara, T.; Fujisawa, K.; Kitajima, N.; Akita, M.; Moro-oka, Y. *Inorg. Chem.* **1997**, *36*, 4539.
- (3) Kitajima, N.; Osawa, M.; Tanaka, M.; Moro-oka, Y. *J. Am. Chem. Soc.* **1991**, *113*, 8952.
- (4) Co complexes: (a) Hikichi, S.; Komatsuzaki, H.; Kitajima, N.; Akita, M.; Mukai, M.; Kitagawa, T.; Moro-oka, Y. *Inorg. Chem.* **1997**, *36*, 266. (b) Hikichi, S.; Komatsuzaki, H.; Akita, M.; Moro-oka, Y. *J. Am. Chem. Soc.* **1998**, *120*, 4699. Co and Ni complexes: (c) Hikichi, S.; Yoshizawa, M.; Sasakura, Y.; Akita, M.; Moro-oka, Y. *J. Am. Chem. Soc.* **1998**, *120*, 10567. Ru complexes; (d) Takahashi, Y.; Akita, M.; Hikichi, S.; Moro-oka, Y. *Inorg. Chem.* **1998**, *37*, 3186. (e) Takahashi, Y.; Akita, M.; Hikichi, S.; Moro-oka, Y. *Organometallics* **1998**, *17*, 4884. Rh complexes: (f) Akita, M.; Ohta, K.; Takahashi, Y.; Hikichi, S.; Moro-oka, Y. *Organometallics* **1997**, *16*, 4121. (g) Takahashi, Y.; Hashimoto, M.; Hikichi, S.; Akita, M.; Moro-oka, Y. manuscript in preparation. Pd complexes: (h) Akita, M.; Miyaji, T.; Hikichi, S.; Moro-oka, Y. *Chem. Commun.* **1998**, 1005.
- (5) Review: (a) Rehder, D. *Angew. Chem., Int. Ed. Engl.* **1991**, *30*, 148. (b) Butler, A.; Clague, M. J.; Meister, G. E. *Chem. Rev.* **1994**, *94*, 625. (c) Slebodnick, C.; Hamstra, B. J.; Pecoraro, V. L. *Struct. Bonding* **1997**, *89*, 51.
- (6) Vanadium haloperoxidase, enzyme: (a) Butler, A.; Walker, J. V. *Chem. Rev.* **1993**, *93*, 1937. (b) Butler, A.; Baldwin, A. H. *Struct. Bonding* **1997**, *89*, 109. (c) Messerschmidt, A.; Prade, L.; Wever, R. *Biol. Chem.* **1997**, *378*, 309. Model complexes: (d) Clague, M. J.; Keder, N. L.; Butler, A. *Inorg. Chem.* **1993**, *32*, 4754. (e) Colpas, G. J.; Hamstra, B. J.; Kampf, J. W.; Pecoraro, V. L. *J. Am. Chem. Soc.* **1996**, *118*, 3469.
- (7) Examples of the oxidation reactions by the vanadium complexes. Enantioselective oxidation: (a) Nakajima, K.; Kojima, M.; Toriumi, K.; Saito, K.; Fujita, J. *Bull. Chem. Soc. Jpn.* **1989**, *62*, 760. (b) Nakajima, K.; Kojima, K.; Kojima, M.; Fujita, J. *Bull. Chem. Soc. Jpn.* **1990**, *63*, 2620. (c) Bolm, C.; Bienewald, F. *Angew. Chem., Int. ed. Engl.* **1995**, *34*, 2640. (d) Schmidt, H.; Bashirpoor, M.; Rehder, D. *J. Chem. Soc., Dalton Trans.* **1996**, 3865. (e) Vetter, A. H.; Berkessel, A. *Tetrahedron Lett.* **1998**, *39*, 1741. Hydrocarbon oxidation: (f) Mimoun, H.; Saussine, L.; Daire, E.; Postel, M.; Fischer, J.; Weiss, R. *J. Am. Chem. Soc.* **1983**, *105*, 3101. (g) Rao, P. R. H. P.; Ramaswamy, A. V. *J. Chem. Soc., Chem. Commun.* **1992**, 1245. (h) Rao, P. R. H. P.; Ramaswamy, A. V.; Ratnasamy, P. *J. Catal.* **1993**, *141*, 604. (i) Bianchi, M.; Bonchio, M.; Conte, V.; Coppa, F.; Di Furia, F.; Modena, G.; Moro, S.; Standen, S. *J. Mol. Catal.* **1993**, *83*, 107. (j) Chang, C. J.; Labinger, J. A.; Gray, H. B. *Inorg. Chem.* **1997**, *36*, 5927.
- (8) Dean, N. S.; Bond, M. R.; O'Connor, C. J.; Carrano, C. J. *Inorg. Chem.* **1996**, *35*, 7643.
- (9) A vanadium(V)–diphenoxo complex, Tp^{Me₂}V(O)(OPh)₂ was hydrolyzed to give a dinuclear hydroxo complex, [Tp^{Me₂}V(O)(OH)]₂(μ-O), although a structure of the hydroxo complex was not revealed: Holmes, S.; Carrano, C. J. *Inorg. Chem.* **1991**, *30*, 1231.
- (10) (a) Kime-Hunt, E.; Spartalian, K.; DeRusha, M.; Nunn, C. M.; Carrano, C. J. *Inorg. Chem.* **1989**, *28*, 4392. (b) Collison, D.; Eardley, D. R.; Mabbs, F. E.; Powell, A. K.; Turner, S. S. *Inorg. Chem.* **1993**, *32*, 664.
- (11) Beddoes, R. L.; Collison, D.; Mabbs, F. E.; Passand, M. A. *Polyhedron* **1990**, *9*, 2483.
- (12) (a) Köppen, M.; Fresen, G.; Wiegardt, K.; Llusar, R. M.; Nuber, B.; Weiss, J. *Inorg. Chem.* **1988**, *27*, 721. (b) Heimer, N. E.; Cleland, W. E., Jr. *Acta Crystallogr.* **1990**, *C46*, 2049. (c) Mohan, M.; Holmes, S. M.; Butcher, R. J.; Jasinski, J. P.; Carrano, C. J. *Inorg. Chem.* **1992**, *31*, 2029. (d) Carrano, C. J.; Verastegue, R.; Bond, M. R. *Inorg. Chem.* **1993**, *32*, 3589. (e) Mokry, L. M.; Thompson, J.; Bond, M. R.; Otieno, T.; Mohan, M.; Carrano, C. J. *Inorg. Chem.* **1994**, *33*, 2705. (f) Sundermeyer, J.; Putterlik, J.; Foth, M.; Field, J. S.; Ramesar, N. *Chem. Ber.* **1994**, *127*, 1201. (g) Carrano, C. J.; Mohan, M.; Holmes, S. M.; de la Rosa, R.; Butler, A.; Charnock, J. M.; Garner, C. D. *Inorg. Chem.* **1994**, *33*, 646. (h) Bond, M. R.; Czernuszewicz, R. S.; Dave, B. C.; Yan, Q.; Mohan, M.; Verastegue, R.; Carrano, C. J. *Inorg. Chem.* **1995**, *34*, 5857. (i) Scheuer, S.; Fischer, J.; Kress, J. *Organometallics* **1995**, *14*, 2627. (j) Collison, D.; Mabbs, F. E.; Turner, S. S.; Powell, A. K.; McInnes, E. J. L.; Yellowless, L. J. *J. Chem. Soc., Dalton Trans.* **1997**, 1201. (k) Dean, N. S.; Mokry, L. M.; Bond, M. R.; Mohan, M.; Otieno, T.; O'Connor, C. J.; Spartalian, K.; Carrano, C. J. *Inorg. Chem.* **1997**, *36*, 1424. (l) Herberhold, M.; Frohmader, G.; Hofmann, T.; Milius, W.; Darkwa, J. *Inorg. Chim. Acta* **1998**, *267*, 19.
- (13) Perrin, D. D.; Armarego, W. L.; Perrin, D. R. *Purification of Laboratory Chemicals*, 2nd ed.; Pergamon: New York, 1980.
- (14) Bristow, S.; Collison, D.; McAvilley, S. C. M.; Clegg, W. *Polyhedron* **1989**, *8*, 87.
- (15) Imai, S.; Fujisawa, K.; Kobayashi, T.; Shirasawa, N.; Fujii, H.; Yoshimura, T.; Kitajima, N.; Moro-oka, Y. *Inorg. Chem.* **1998**, *37*, 3066.

(V=O). FD-MS (*m/z*, relative intensity): 719 (100%; 1⁺), 567 (57%; 1-Pz^{Pr₂}H). UV-vis (toluene, nm, ε/M⁻¹cm⁻¹): 769 (40), 601 (22).

Tp^{Pr₂}V(O)(Cl)(py) (2). KTp^{Pr₂} (6.0 × 10² mg; 1.2 mmol) and VOCl₂(MeCN)₂(H₂O) (2.9 × 10² mg; 1.2 mmol) were stirred in 10 mL of pyridine for 5 min at room temperature. After removal of the volatiles under vacuum, the resulting solid was extracted with pentane. Concentration of the blue pentane extract followed by refrigeration at -20 °C afforded blue precipitates, which were collected by filtration. Then, the resulting blue solid of **2** was washed with a minimal amount of pentane and dried under vacuum (46 mg; 7.1 × 10⁻² mmol; 5.8% yield). Anal. Calcd for C₃₂H₅₁N₇OBClV: C, 59.40; H, 7.95; N, 15.15; Cl, 5.48. Found: C, 59.09; H, 8.30; N, 14.98; Cl, 5.42. IR (KBr pellet, ν/cm⁻¹): 2554 (BH), 1605 (pyridine C=N or C=C), 1537 (Tp^{Pr₂}-pyrazolyl C=N), 975 (V=O). FD-MS (*m/z*, relative intensity): 567 (100%, 2⁻py). UV-vis (toluene, nm, ε/M⁻¹cm⁻¹): 756 (53), 588 (36), 360 (560).

Tp^{Pr₂}V(O)(acac) (3). KTp^{Pr₂} (1.0 × 10³ mg; 2.0 mmol) and VO(acac)₂ (5.2 × 10² mg; 2.0 mmol) were dissolved in 50 mL of toluene. The reaction mixture was stirred for 5 h at 50 °C. After removal of the solvent under vacuum, the resulting solid was extracted with pentane. Concentration of the blue pentane extract followed by refrigeration at -20 °C afforded blue precipitate of **3** (56 mg; 8.9 × 10⁻² mmol; 4.4% yield). Anal. Calcd for C₃₂H₅₃N₆O₃BV: C, 60.86; H, 8.46; N, 13.31. Found: C, 60.54; H, 8.37; N, 13.26. IR (KBr pellet, ν/cm⁻¹): 2540 (BH), 1580 (acac C=O), 1520 (Tp^{Pr₂}-pyrazolyl C=N), 967 (V=O). FD-MS (*m/z*, relative intensity): 631 (100%; 3⁺). UV-vis (toluene, nm, ε/M⁻¹cm⁻¹): 770 (48), 556 (15), 408 (54), 395 (56).

Tp^{Pr₂}V(O)(OH)(OH₂) (4). A toluene solution (30 mL) of **1** (1.0 × 10³ mg; 1.4 mmol) was stirred with 10 equiv of an aqueous NaOH (0.1M, 14 mL) for 1 h. After removal of the water layer, the toluene phase was dried over Na₂SO₄ and then filtered. Evaporation of toluene under vacuum gave purple solid. The purple solid was suspended in 10 mL of MeCN. After the purple suspension was stirred overnight in order to remove byproducts, a purple solid was collected by filtration and then washed with a minimal amount of MeCN. The resulting purple compound was dissolved in 10 mL of CH₂Cl₂. Then, the purple CH₂-Cl₂ solution was concentrated under vacuum and cooled at -20 °C, and **4** was obtained as purple microcrystalline solid (4.6 × 10² mg; 8.2 × 10⁻¹ mmol; 57% yield). Similar treatment of **2** (30 mg; 4.6 × 10⁻² mmol) also yielded **4** (17 mg; 3.0 × 10⁻² mmol; 65% yield). Anal. Calcd for C₂₇H₄₉N₆O₃BV: C, 57.15; H, 8.70; N, 14.81. Found: C, 57.39; H, 8.59; N, 15.21. IR (KBr pellet, ν/cm⁻¹): 3682, 3620 (OH), 2543 (BH), 1537 (Tp^{Pr₂}-pyrazolyl C=N), 978 (V=O); (CH₂Cl₂ film, ν/cm⁻¹): 3676, 3620 (OH), 2549 (BH), 1537 (Tp^{Pr₂}-pyrazolyl C=N), 971 (V=O). FD-MS (*m/z*, relative intensity): 1081 (100%; (4-H₂O)₂-OH). UV-vis (toluene, nm, ε/M⁻¹cm⁻¹): 724 (18), 551 (19).

Trinuclear bis(μ-hydroxo)-bis(μ-pyrazolato) complex, Tp^{Pr₂}V(O)(μ-OH)(μ-Pz^{Pr₂})V(O)(μ-OH)(μ-Pz^{Pr₂})V(O)(Tp^{Pr₂}) (5). The crude purple solid of **4** (1.2 × 10² mg), which was obtained by reaction of the toluene solution of **1** (1.3 × 10² mg; 1.9 × 10⁻¹ mmol) with the aqueous NaOH followed by workup as indicated above, was heated at 80 °C for 6 h under vacuum. The resulting solid was extracted with pentane. After removal of pentane under vacuum, a bluish purple solid was recrystallized from CH₂Cl₂ at -20 °C (43 mg; 2.9 × 10⁻² mmol; 47% yield (based on **1**)). Anal. Calcd for C₇₂H₁₂₄N₁₆O₅B₂V₃: C, 58.90; H, 8.51; N, 15.26. Found: C, 59.00; H, 8.26; N, 15.48. IR (KBr pellet, ν/cm⁻¹): 3630 (OH), 2543 (BH), 1536 (Tp^{Pr₂}-pyrazolyl C=N), 1523 (pyrazolate C=N), 981, 975 (V=O); (CH₂Cl₂ film, ν/cm⁻¹): 3632 (OH), 2549 (BH), 1537 (Tp^{Pr₂}-pyrazolyl C=N), 1524 (pyrazolate C=N), 977 (br, V=O). FD-MS (*m/z*, relative intensity): 1467 (100%; 5⁺). UV-vis (toluene, nm, ε/M⁻¹cm⁻¹): 709 (100), 533 (59).

Tp^{Me₂}V(O)(Cl)(NCMe) (6). NaTp^{Me₂} (1.3 × 10³ mg; 4.0 mmol) was added to an MeCN solution (50 mL) of VOCl₂(MeCN)₂(H₂O) (9.6 × 10² mg; 4.0 mmol), and this reaction mixture was stirred for 1 h at 50 °C. After removal of the solvent under vacuum, the resulting solid was extracted with CH₂Cl₂. Evaporation of CH₂Cl₂ followed by crystallization from MeCN at -20 °C afforded blue crystals of **6** (1.2 × 10³ mg; 2.7 mmol; 67% yield). Anal. Calcd for C₁₇H₂₅N₇OBClV: C, 46.34; H, 5.72; N, 22.25; Cl, 8.05. Found: C, 45.83; H, 5.63; N, 22.12; Cl, 7.61. IR (KBr pellet, ν/cm⁻¹): 2543 (BH), 2315, 2289, 2249 (acetonitrile C≡N), 1543 (Tp^{Me₂}-pyrazolyl C=N), 966 (V=O). FD-MS (*m/z*,

relative intensity): 399 (100%; 6-MeCN). UV-vis (MeCN, nm, ε/M⁻¹cm⁻¹): 756 (39), 600 (sh, 12). (toluene): 735 (130), 370 (sh, 620).

Reaction of VOCl₂ with NaTp^{Me₂} (Formation of Tp^{Me₂}V(O)(Cl)-(Pz^{Me₂}H)). A THF solution (10 mL) of NaTp^{Me₂} (4.5 × 10² mg; 1.4 mmol) was added to a MeOH suspension (40 mL) of VOCl₂ (2.1 × 10² mg; 1.5 mmol), and the solvents were removed immediately under vacuum. The resulting solid was extracted with MeCN. After concentration of the MeCN solution, recrystallization at -20 °C afforded a blue solid (2.3 × 10² mg; 4.7 × 10⁻¹ mmol; 31% yield). The blue product was identified as the pyrazole-containing complex, Tp^{Me₂}V(O)(Cl)(Pz^{Me₂}H), by comparison with the previously reported data.^{10b} IR (KBr pellet, ν/cm⁻¹): 3306 (pyrazole NH), 2538 (BH), 1575 (pyrazole C=N), 1543 (Tp^{Me₂}-pyrazolyl C=N), 964 (V=O). FD-MS (*m/z*, relative intensity): 495 (100%; [Tp^{Me₂}V(O)(Cl)(Pz^{Me₂}H)]⁺).

Hydrolysis of Tp^{Me₂}V(O)(Cl)(NCMe) (6) (Formation of (κ³-Tp^{Me₂})V(O)(μ-OH)₂V(O)(κ²-Tp^{Me₂}) (7) and the Pink Hydroxo Complex 8). A CH₂Cl₂ solution (40 mL) of **6** (8.7 × 10² mg; 2.0 mmol) was stirred with 1 equiv of an aqueous NaOH (0.1 M, 20 mL) for 10 min. After removal of the water layer, the resulting purple suspension was filtered through a glass filter to separate the insoluble pink precipitate **8**. The filtrate was evaporated under vacuum giving bluish purple solid. Recrystallization from a mixture of CH₂Cl₂ and pentane afforded **7** (3.0 × 10² mg; 4.0 × 10⁻¹ mmol; 40% yield) as bluish purple crystals. Separated pink solid **8** was washed with MeCN, H₂O, and toluene (1.7 × 10² mg; 4.4 × 10⁻¹ mmol as Tp^{Me₂}V(O)(OH)(OH₂), 22% yield).

Spectroscopic data for **7**: Anal. Calcd for C₃₀H₄₆N₁₀O₄B₂V₂: C, 47.27; H, 6.08; N, 22.05. Found: C, 47.93; H, 6.24; N, 21.38. IR (KBr pellet, ν/cm⁻¹): 3635 (OH), 3539 (br, OH), 2520 (BH), 1543 (Tp^{Me₂}-pyrazolyl C=N), 981, 958 (V=O); (CH₂Cl₂ film): 3629 (OH), 2545, 2527 (BH), 1543 (Tp^{Me₂}-pyrazolyl C=N), 983, 955 (V=O). FD-MS (*m/z*, relative intensity): 762 (7.6%; 7⁺), 745 (100%; 7-OH). UV-vis (toluene, nm, ε/M⁻¹cm⁻¹): 759 (139), 639 (157), 536 (135).

Spectroscopic data for **8**: Anal. Calcd for C₁₅H₂₅N₆O₃BV (Tp^{Me₂}V(O)(OH)(OH₂)): C, 45.14; H, 6.31; N, 21.05. Found: C, 45.58; H, 6.36; N, 21.16. IR (KBr pellet, ν/cm⁻¹): 3657, 3603 (OH), 2514 (BH), 1542 (Tp^{Me₂}-pyrazolyl C=N), 979 (V=O).

An MeCN solution (30 mL) of **6** (1.0 × 10³ mg; 2.3 mmol) and a 0.5 M aqueous NaOH (2.0 mL) solution was stirred for 5 min. Washing the resulting pink precipitate with MeCN, H₂O, and toluene afforded **8** (6.6 × 10² mg; 1.7 mmol as Tp^{Me₂}V(O)(OH)(OH₂), 74% yield). Isolated **8** was well-dried under vacuum and then extracted with CH₂-Cl₂. Recrystallization from CH₂Cl₂/pentane yielded **7** (3.3 × 10² mg; 4.3 × 10⁻¹ mmol; 54% yield) as a bluish purple crystalline solid. Treatment of a toluene solution of **6** with the aqueous NaOH (0.5 M) also afford **8** but not **7**.

Attempt at preparation of a chloro complex with Tp^{Bu^f,Pr^f}. KTp^{Bu^f,Pr^f} was added to a MeCN solution of VOCl₂(MeCN)₂(H₂O), and then the reaction mixture was stirred at room temperature. After workup in manners similar to the preparation of **1**, **2**, and **6**, an IR spectrum of the resulting solid was measured. In any case, no peak arising from BH vibration was observed. Further characterization was not performed.

X-ray Data Collections and Structural Determinations. Conditions (solvent, temperature; under Ar unless otherwise stated) for crystallizations were as follows. **1** (hexane, r.t., air), **2**·Et₂O (ether, r.t., air), **3** (hexane, r.t., air), **4**·2Et₂O (ether, -40 °C), **5**·2Et₂O (ether, -40 °C), **6**·2MeCN (acetonitrile, -20 °C), **7**·CH₂Cl₂ (dichloromethane, -20 °C). The crystals of **1**, **2**·Et₂O, and **3** were mounted on glass fibers, and the other crystals were sealed in thin-wall glass capillaries.

Diffraction measurements of **1**, **2**·Et₂O, **3**, **4**·2Et₂O, and **5**·2Et₂O were made on a Rigaku RAXIS IV imaging plate area detector with Mo Kα radiation (λ = 0.710 69 Å). Indexing was performed from three oscillation images that were exposed for 5 min. The crystal-to-detector distances were 110 mm (**1**, **3**, and **4**·2Et₂O) or 120 mm (**2**·Et₂O and **5**·2Et₂O). Data collection parameters were as follows: the oscillation range, 5° (**1**), 4.5° (**3**), 3° (**2**·Et₂O, **4**·2Et₂O and **5**·2Et₂O); number of oscillation images, 18 (**1**), 20 (**3**), 30 (**2**·Et₂O, **4**·2Et₂O and **5**·2Et₂O); the exposed time, 150 min (**1**), 125 min (**3**), 75 min (**2**·Et₂O), 15 min (**4**·2Et₂O), 30 min (**5**·2Et₂O). All the data collections were carried out

Table 1. Crystal Data and Data Collection Details of **1**, **2**·Et₂O, **3**, **4**·2Et₂O, **5**·2Et₂O, **6**·2MeCN, and **7**·CH₂Cl₂

complex	1	2 ·Et ₂ O	3	4 ·2Et ₂ O	5 ·2Et ₂ O	6 ·2MeCN	7 ·CH ₂ Cl ₂
formula	VClO ₂ N ₈ C ₃₆ BH ₆₂	VClO ₂ N ₇ C ₃₆ BH ₆₁	VO ₃ N ₆ C ₃₂ BH ₅₃	VO ₅ N ₆ C ₃₅ BH ₆₉	V ₃ O ₇ N ₁₆ C ₈₀ B ₂ H ₁₄₄	VClO ₂ N ₉ C ₂₁ BH ₃₁	V ₂ Cl ₂ O ₄ N ₁₂ C ₃₁ B ₂ H ₄₈
formula wt	720.14	721.13	631.56	715.72	1616.57	522.74	847.21
crystal system	orthorhombic	monoclinic	monoclinic	orthorhombic	monoclinic	monoclinic	triclinic
space group	<i>Fdd2</i> (# 43)	<i>P21/a</i> (# 14)	<i>P21/c</i> (# 14)	<i>Pbca</i> (# 61)	<i>P21/n</i> (# 14)	<i>P21/n</i> (# 14)	<i>P1</i> (# 2)
<i>a</i> /Å	33.518(4)	16.428(8)	16.776(5)	18.382(6)	12.252(6)	16.115(7)	12.617(4)
<i>b</i> /Å	36.38(1)	24.743(5)	12.444(3)	25.810(3)	44.222(6)	15.672(8)	14.345(7)
<i>c</i> /Å	13.445(2)	9.881(2)	18.980(2)	18.275(2)	17.301(2)	10.826(5)	12.324(3)
α /deg	90	90	90	90	90	90	94.04(3)
β /deg	90	105.47(3)	113.99(1)	90	97.78(3)	98.33(4)	105.42(2)
γ /deg	90	90	90	90	90	90	106.14(3)
<i>V</i> /Å ³	16396(5)	3870(2)	3620(1)	8670(2)	9287(4)	2705(4)	2040(3)
<i>Z</i>	16	4	4	8	4	4	2
<i>D</i> (calcd.)/g·cm ⁻³	1.17	1.24	1.16	1.10	1.16	1.28	1.38
crystal size/mm	0.05 × 0.05 × 0.07	0.2 × 0.2 × 0.25	0.02 × 0.05 × 0.1	0.35 × 0.3 × 0.07	0.1 × 0.1 × 0.15	0.1 × 0.2 × 0.08	0.15 × 0.2 × 0.1
data collection temp/°C	-60	-60	-60	-60	-60	-60	-65
diffractometer	Rigaku RAXIS-IV	Rigaku RAXIS-IV	Rigaku RAXIS-IV	Rigaku RAXIS-IV	Rigaku RAXIS-IV	Rigaku AFC-5S	Rigaku AFC-5S
μ (Mo K α)/cm ⁻¹	3.44	3.65	3.12	2.70	3.52	4.96	6.39
2θ range/deg	-55.0	-51.3	-55.0	-53.9	-49.1	3-50.0	2.8-50.0
no. of measd reflectns	4416	6087	4923	8859	11271	5140	7548
no. of obsd reflectns (<i>I</i> > 3.0 σ (<i>I</i>))	3499	4658	3227	6252	10075	3687	4447
no. of parameters refined	452	409	397	452	973	307	486
<i>R</i> /%	4.75	6.72	6.75	6.79	5.91	4.68	5.72
<i>R_w</i> /%	4.46	7.31	6.82	7.69	6.20	5.11	6.13

at -60 °C. Readout was performed with the pixel size of 100 μ m × 100 μ m. The data processing was performed on an IRIS Indy computer.

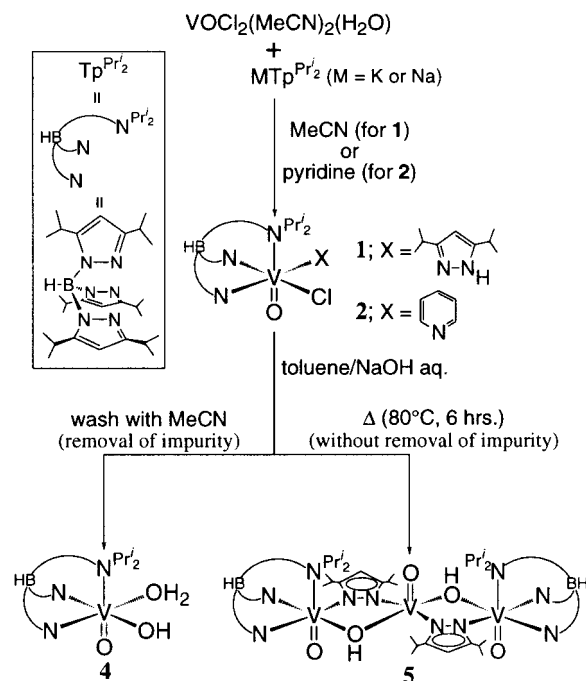
Diffraction measurements of **6**·2MeCN and **7**·CH₂Cl₂ were made on a Rigaku AFC-5S automated four-circle diffractometer. A Mo X-ray source equipped with a graphite monochromator (Mo K α , λ = 0.710 680 Å) was used. Automatic centering and least-squares routines were carried out for all the compounds with 20 reflections of 20° < 2 θ < 25° to determine the cell parameters. Data collections were completed with ω -2 θ scan.

Crystallographic data and the results of refinements are summarized in Table 1. Structure analysis was performed on an IRIS O2 computer by using the teXsan structure solving program package obtained from Rigaku Corp., Tokyo, Japan. The structures of the complexes were solved by the direct methods (SHELXS-86). Subsequent difference Fourier synthesis (DIRDIF) easily located all the non-hydrogen atoms, which were refined anisotropically except the disordered Et₂O solvates in **2**·Et₂O and **4**·2Et₂O. Neutral scattering factors were obtained from the standard source.¹⁶ All hydrogen atoms except those attached to the disordered isopropyl group (in **1** and **3**), the Et₂O molecules (in **2**·Et₂O and **4**·2Et₂O), and the oxygen atoms of the aqua and hydroxo groups in **4**·2Et₂O and **7**·CH₂Cl₂ were located at the calculated positions and were not refined (*d*(C-H) = 0.95 Å with the isotropic thermal factor of *U*_{iso}(H) = 1.2*U*_{iso}(C)). The hydrogen atoms of the hydroxo and aqua groups in **4**·2Et₂O and **7**·CH₂Cl₂ were refined isotropically. Full interatomic distances, bond angles, atomic coordinates, and isotropic and anisotropic thermal parameters are available as Supporting Information.

Results and Discussion

1. Synthesis of Chloro and Hydroxo Complexes of VO²⁺ with Tp^{Pr₂}. Previously, we reported the synthesis of divalent metal hydroxo complexes with the Tp^{Pr₂} and Tp^{Buⁱ,Prⁱ} ligands via hydrolysis of the corresponding halo, nitrate, and carboxylato complexes, which were prepared by the reaction of appropriate metal salts with KTp^{Pr₂} and KTp^{Buⁱ,Prⁱ}.² Although formal charge of the vanadium center in vanadyl ion (VO²⁺) is +4, the VO²⁺ fragment can be regarded as a divalent cation from the viewpoint of metal-complex synthesis.¹⁷ Thus, we expected that a ligand exchange reaction between the alkali metal salts of Tp^R ligands

Scheme 1



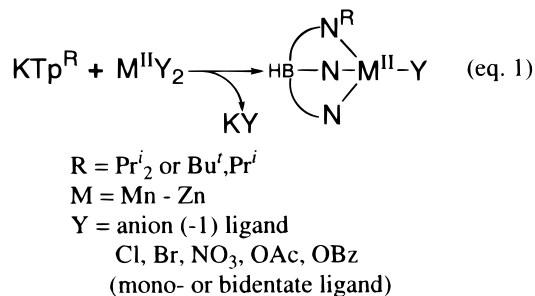
and appropriate VO²⁺ precursors followed by hydrolysis might yield the desired hydroxo complex.² In fact, we succeeded in preparation of chloro complexes Tp^{Pr₂}V(O)Cl(X) (**1**, X = Pz^{Pr₂}H; **2**, X = py) and subsequent hydroxylation of these complexes as summarized in Scheme 1.

(a) Chloro Complexes 1 and 2. Previously, two types of six-coordinate octahedral VO²⁺-chloro complexes with the less hindered Tp^{Me₂} ligand, Tp^{Me₂}V(O)Cl(X) (X = neutral nitrogen or oxygen donor ligand), have been reported. One type is the DMF adducts, Tp^{Me₂}V(O)Cl(DMF), which is obtained by oxidation of an air-sensitive V(III) dichloro complex, Tp^{Me₂}-

(16) *International Tables for X-ray Crystallography*; Kynoch Press: Birmingham, 1975; Vol. 4.

(17) Cotton, F. A.; Wilkinson, G. *Advanced Inorganic Chemistry*, 5th ed.; Wiley: New York, 1988.

VCl₂(DMF).^{10a} The other octahedral V(IV) chloro complex, Tp^{Me₂}V(O)Cl(Pz^{Me₂}H), has been obtained by a direct ligand exchange reaction between VOCl₂(MeCN)₂(H₂O) and KTp^{Me₂}.^{10b} The common problem of synthesis of these chloro complexes is the relatively low yields of the desired complexes due to decomposition of the Tp^R moiety during the displacement processes, giving free pyrazoles and/or its vanadium complexes.^{10a,18} In this study, we adopted the direct ligand exchange method because handling of vanadium(IV) compounds should be easier than that of more air-sensitive vanadium(III) compounds, and halo and carboxylato complexes of first-row divalent metal ions with the Tp^R (R = Prⁱ₂ or Bu^t, Prⁱ) ligands reported by us had been prepared by a similar direct ligand exchange method as shown in eq 1.²



Reaction of an acetonitrile solution of VOCl₂(MeCN)₂(H₂O) with KTp^{Prⁱ}₂ yielded a pyrazole-containing chloro complex **1**, Tp^{Prⁱ}₂V(O)Cl(Pz^{Prⁱ}₂H) (Pz^{Prⁱ}₂H = 3,5-diisopropylpyrazole), as found for the Tp^{Me₂} derivative Tp^{Me₂}V(O)Cl(Pz^{Me₂}H).^{10b} A very strong absorption at 3431 cm⁻¹ (νN-H) in an IR spectrum of **1** is characteristic of the coordinating pyrazole ligand.^{2d,e,19} The molecular structure of **1** was determined by X-ray crystallographic analysis (Figure 1 and Table 2). The vanadium center has a six-coordinate octahedral geometry containing an N₃Cl₁ basal plane. The additional pyrazole ligand occupies an equatorial position. The overall molecular structure of **1** is almost identical with those of the other chloro complexes, Tp^RV(O)Cl(X), obtained in this study (see below) and previously,¹⁰ although the supporting Tp^R ligands and the neutral N or O atom donor ligands are varied. According to the previous Carrano and co-workers' report, introduction of the bulky 3-isopropyl- and 3-*tert*-butyl groups to the pyrazolyl rings of the Tp^R ligands (i.e., Tp^{Prⁱ} = hydrotris(3-isopropyl-1-pyrazolyl)borate and Tp^{Bu^t} = hydrotris(3-*tert*-butyl-1-pyrazolyl)borate) hampers the formation of the corresponding Tp^RV complexes and instead results in breaking of the B-N bonds of Tp^R to give the pyrazole complexes of vanadium.^{10a,18} In contrast, we succeeded in getting the desired complex having the sterically demanding Tp^{Prⁱ}₂ ligand. It is known that the B-N bonds of Tp^{3R,5R'} with the 3,5-dialkylpyrazolyl groups are more resistant toward hydrolysis than those of the Tp^{3R} (hydrotris(3-R-1-pyrazolyl)borate) analogues since three substituents on the 5-positions of the pyrazolyl groups form a hydrophobic pocket around the B atom.^{1b} The hydrophobic shading pocket might make the isolation of Tp^{Prⁱ}₂V(O)Cl(X) possible, although it could not perfectly inhibit the decomposition of the Tp^{Prⁱ}₂ ligand. Addition of the pyrazole ligand was not effective for increase of the product yield. Use of a sodium salt of Tp^{Prⁱ}₂ instead of

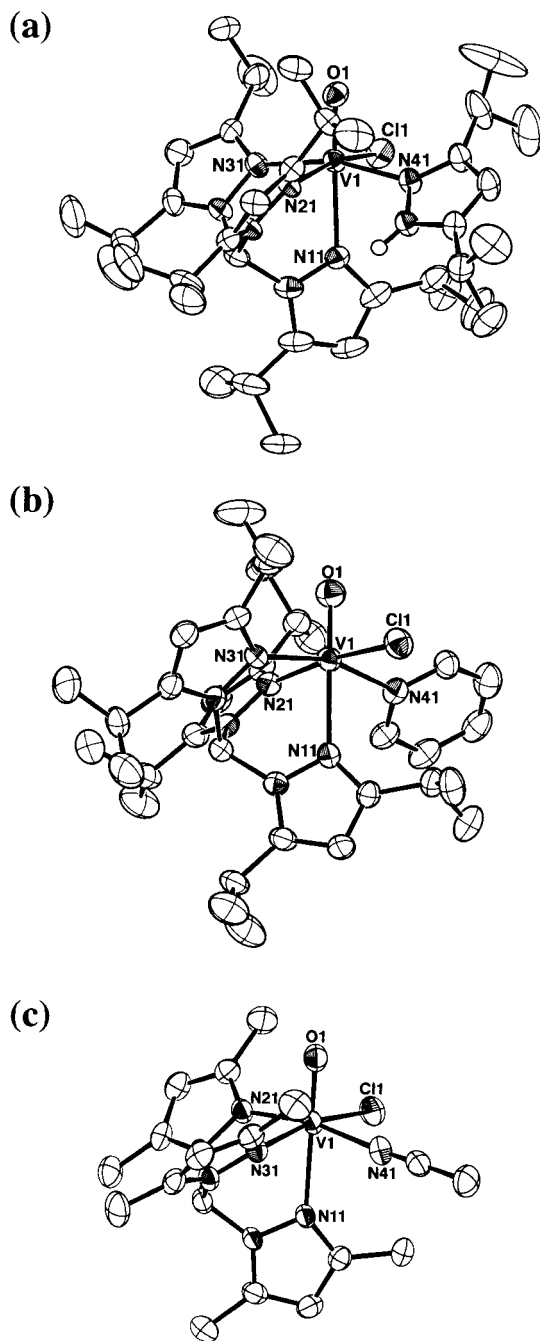


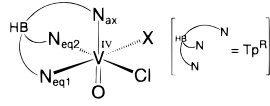
Figure 1. ORTEP drawing of a series of chloro complexes **1**, **2**·Et₂O, and **6**·2MeCN (drawn at the 50% probability level). All hydrogen atoms except that attached to the nitrogen atom of the coordinating pyrazole ligand in **3** and the solvent molecules in **2**·Et₂O and **6**·2MeCN are omitted for clarity. (a) Tp^{Prⁱ}₂V(O)Cl(Pz^{Prⁱ}₂H) (**1**). The disordered carbon atoms of one of the three 5-Prⁱ groups in the Tp^{Prⁱ}₂ ligand are omitted for clarity. (b) Tp^{Prⁱ}₂V(O)Cl(py) (**2**). (c) Tp^{Me₂}V(O)Cl(NCMe) (**6**).

KTp^{Prⁱ}₂ also resulted in the formation of the pyrazole adduct **1** (not a MeCN adduct), although an MeCN-containing chloro complex, Tp^{Me₂}V(O)Cl(NCMe) (**6**), was obtained under the same reaction conditions in our Tp^{Me₂} system (vide infra).

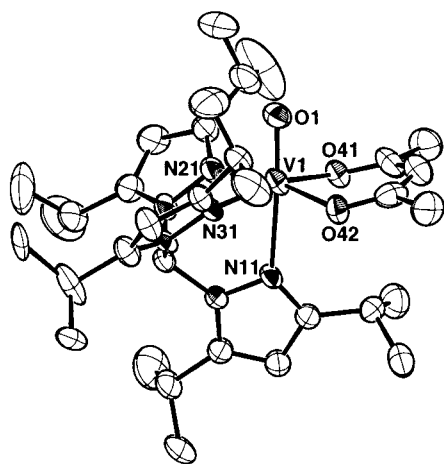
Reaction of VOCl₂(MeCN)₂(H₂O) and KTp^{Prⁱ}₂ in pyridine yielded a pyridine-containing chloro complex **2**, Tp^{Prⁱ}₂V(O)Cl(py). An IR spectrum of **2** contained a peak at 1605 cm⁻¹ that was assigned to the C=C or/and C=N vibration of the metal-coordinating pyridine molecule. The molecular structure of **2** was also revealed by X-ray crystallographic analysis (Figure 1

(18) Structures of several vanadium-pyrazole complexes have been reported: Mohan, M.; Bond, M. R.; Otieno, T.; Carrano, C. J. *Inorg. Chem.* **1995**, *34*, 1233.

(19) Kitajima, N.; Komatsuzaki, H.; Hikichi, S.; Osawa, M.; Moro-oka, Y. *J. Am. Chem. Soc.* **1994**, *116*, 11596.

Table 2. Selected Bond Lengths (Å) and Angles (deg) for $\text{Tp}^{\text{Pr}'}\text{V}(\text{O})(\text{Cl})(\text{X})$


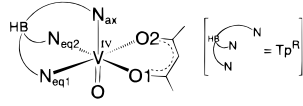
	$\text{Tp}^{\text{Pr}'}_2$ complexes		Tp^{Me_2} complexes		
	1 X = $\text{Pz}^{\text{Pr}'}_2\text{H}$	2 · Et_2O X = py	8 · 2MeCN X = NCMc	DMF adduct ^{10a} X = DMF	$\text{Pz}^{\text{Me}_2}\text{H}$ adduct ^{10b} X = $\text{Pz}^{\text{Me}_2}\text{H}$
	Bond Lengths (Å)				
V–Cl	2.338(2)	2.364(1)	2.354(1)	2.354(2)	2.377(2)
V=O	1.638(4)	1.618(3)	1.628(2)	1.649(5)	1.599(4)
V–X	2.174(4)	2.174(4)	2.123(3)	2.043(4)	2.136(5)
V– N_{ax}	2.326(4)	2.324(4)	2.316(3)	2.329(6)	2.355(4)
V– $\text{N}_{\text{eq}1}$	2.082(4)	2.107(4)	2.089(3)	2.117(5)	2.107(6)
V– $\text{N}_{\text{eq}2}$	2.125(4)	2.103(4)	2.113(3)	2.110(5)	2.107(4)
	Bond Angles (deg)				
Cl–V–O	97.3(1)	93.7(1)	98.12(9)	98.5(2)	98.3(1)
Cl–V–X	94.9(1)	92.1(1)	89.69(9)	91.5(1)	92.7(1)
Cl–V– N_{ax}	86.1(1)	88.0(1)	87.24(7)	85.7(1)	86.0(1)
Cl–V– $\text{N}_{\text{eq}1}$	90.8(1)	95.5(1)	91.11(8)	92.2(2)	91.8(1)
Cl–V– $\text{N}_{\text{eq}2}$	167.3(1)	173.0(1)	167.49(8)	165.0(2)	165.8(1)
O–V–X	94.6(2)	96.5(2)	93.6(1)	96.7(2)	95.0(2)
O–V– N_{ax}	174.3(2)	176.8(2)	173.7(1)	175.8(2)	175.6(2)
O–V– $\text{N}_{\text{eq}1}$	99.7(2)	100.2(2)	97.7(1)	94.8(2)	95.8(2)
O–V– $\text{N}_{\text{eq}2}$	95.2(2)	93.3(2)	94.4(1)	96.6(2)	95.8(2)
X–V– N_{ax}	80.5(1)	80.7(1)	83.0(1)	83.6(2)	84.1(2)
X–V– $\text{N}_{\text{eq}1}$	163.9(2)	161.1(1)	168.4(1)	167.4(2)	167.6(2)
X–V– $\text{N}_{\text{eq}2}$	86.6(2)	86.2(1)	89.7(1)	87.2(2)	87.7(2)
N_{ax} –V– $\text{N}_{\text{eq}1}$	84.9(2)	82.3(1)	85.5(1)	84.7(2)	84.7(2)
N_{ax} –V– $\text{N}_{\text{eq}2}$	81.7(2)	85.0(1)	80.28(10)	79.2(2)	79.9(1)
$\text{N}_{\text{eq}1}$ –V– $\text{N}_{\text{eq}2}$	84.5(2)	84.1(1)	87.1(1)	86.1(2)	85.1(2)

**Figure 2.** ORTEP drawing of $\text{Tp}^{\text{Pr}'}\text{V}(\text{O})(\text{O})(\text{acac})$ (**3**) (drawn at the 50% probability level). The disordered carbon atoms of one of the three 5- Pr' groups in the $\text{Tp}^{\text{Pr}'}_2$ ligand are omitted for clarity.

and Table 2). However, yield of **2** was quite low and a free $\text{Pz}^{\text{Pr}'}_2\text{H}$ was detected as a byproduct. We thus conclude that partial decomposition of $\text{Tp}^{\text{Pr}'}_2$ is the main reason for the extremely low yield of **2**.

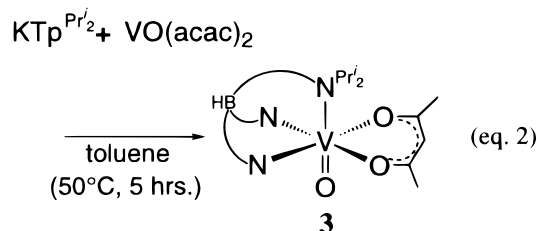
An acetylacetonato complex, $\text{Tp}^{\text{Pr}'}\text{V}(\text{O})(\text{O})(\text{acac})$ (**3**), was also prepared because the Tp^{Me_2} derivative, $\text{Tp}^{\text{Me}_2}\text{V}(\text{O})(\text{O})(\text{acac})$, was previously synthesized via a direct ligand exchange between KTp^{Me_2} and $\text{VO}(\text{acac})_2$.¹¹ Displacement of $\text{V}(\text{O})(\text{O})(\text{acac})_2$ by $\text{KTp}^{\text{Pr}'}_2$ proceeded very slowly, and the desired acetylacetonato complex **3** was obtained only in a very low yield (<5%) (eq 2). However, characterization of **3** was completed by X-ray crystallography (Figure 2 and Table 3) as well as IR, UV–vis, and mass spectroscopy.

(b) Hydroxo Complexes 4 and 5. Recently, the dinuclear bis(μ -hydroxo) complex of VO^{2+} with the less hindered Tp^{H_2}

Table 3. Selected Bond Lengths (Å) and Angles (deg) for $\text{Tp}^{\text{Pr}'}\text{V}(\text{O})(\text{acac})$


	$\text{Tp}^{\text{Pr}'}_2$	Tp^{Me_2}
	3	$\text{Tp}^{\text{Me}_2}\text{V}(\text{O})(\text{acac})$ ¹¹
	Bond Lengths (Å)	
V–O1	1.991(4)	2.013(1)
V–O2	1.970(4)	2.004(1)
V=O	1.626(4)	1.596(2)
V– N_{ax}	2.329(4)	2.328(2)
V– $\text{N}_{\text{eq}1}$	2.108(5)	2.111(2)
V– $\text{N}_{\text{eq}2}$	2.108(5)	2.120(2)
	Bond Angles (deg)	
O1–V–O2	89.0(2)	86.8(1)
O1–V–O	97.7(2)	96.9(1)
O1–V– N_{ax}	84.3(2)	86.7(1)
O1–V– $\text{N}_{\text{eq}1}$	90.0(2)	92.2(1)
O1–V– $\text{N}_{\text{eq}2}$	166.5(2)	<i>a</i>
O2–V–O	96.9(2)	97.2(1)
O2–V– N_{ax}	86.6(2)	85.9(1)
O2–V– $\text{N}_{\text{eq}1}$	168.3(2)	<i>a</i>
O2–V– $\text{N}_{\text{eq}2}$	91.4(2)	91.0(1)
O–V– N_{ax}	176.0(2)	175.4(1)
O–V– $\text{N}_{\text{eq}1}$	94.8(2)	96.0(1)
O–V– $\text{N}_{\text{eq}2}$	95.6(2)	94.9(1)
N_{ax} –V– $\text{N}_{\text{eq}1}$	81.7(2)	81.0(1)
N_{ax} –V– $\text{N}_{\text{eq}2}$	82.3(2)	81.5(1)
$\text{N}_{\text{eq}1}$ –V– $\text{N}_{\text{eq}2}$	86.9(2)	87.4(1)

^a Not reported in the literature (ref 11).



ligand, $[\text{Tp}^{\text{H}_2}\text{V}(\text{O})(\mu\text{-OH})_2]$, has been prepared by hydrolysis of $\text{Tp}^{\text{H}_2}\text{V}(\text{O})(\text{Cl})(\text{DMF})_2$, and its structure is similar to those of a series of the hydroxo complexes bearing the $\text{Tp}^{\text{Pr}'}_2$ ligand, $[\text{Tp}^{\text{Pr}'}_2\text{M}^{\text{II}}(\mu\text{-OH})_2]$ ($\text{M} = \text{Mn to Ni}$),^{4a} although the metal centers in $[\text{Tp}^{\text{H}_2}\text{V}(\text{O})(\mu\text{-OH})_2]$ take a six-coordinate octahedral geometry, involving a terminal oxo ligand.⁸ In this study, VO^{2+} hydroxo complexes with $\text{Tp}^{\text{Pr}'}_2$ were obtained by hydrolysis of the six-coordinate chloro complexes **1** and **2**, whereas the acetylacetonato complex **3** did not react with an aqueous NaOH. Remarkably, structures of the prepared hydroxo complexes were different from those of the previously reported Tp^{H_2} derivative⁸ and the other divalent metal hydroxo complexes with Tp^{Me_2} and $\text{Tp}^{\text{Pr}'}_2$.²

A blue toluene solution of **1** or **2** reacted with the aqueous NaOH solution to give the same purple complex **4**, indicating dissociation of the N-donor, although partial decomposition of the chloro complexes also proceeded during the hydrolysis reaction (see below). After removal of the water layer and the solvent, a resulting solid was washed with MeCN and recrystallized from CH_2Cl_2 to give the pure purple crystalline solid of **4**. An IR spectrum of the solid state **4** exhibited a single $\text{V}=\text{O}$ vibration at 978 cm^{-1} , implying that **4** was a mononuclear complex or a symmetrical multinuclear complex. However, two sharp $\nu\text{O}-\text{H}$ peaks at 3682 and 3620 cm^{-1} were observed.

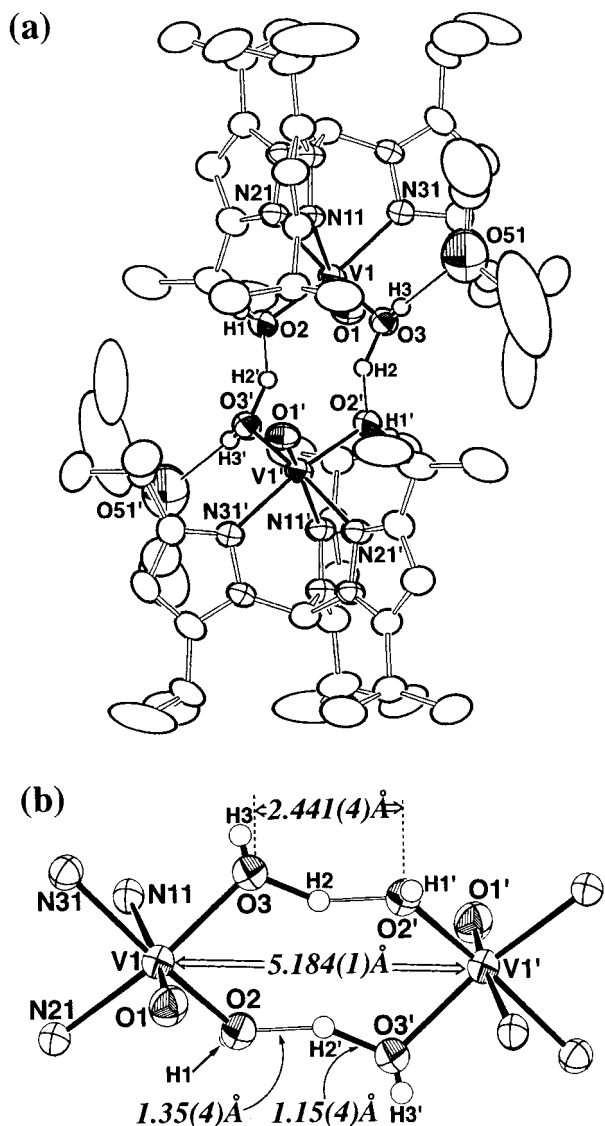


Figure 3. ORTEP drawing of Tp^{Pr₂}V(O)(OH)(OH₂)·2Et₂O (4·2Et₂O) (drawn at the 50% probability level). (a) Dimerized structure of **4**, including intermolecular hydrogen-bonding contacts. All hydrogen atoms, except those attached to the oxygen atoms of the hydroxo and aqua ligands and the noncontacted one Et₂O molecule, are omitted for clarity. (b) Expanded view of the metal centers of the dimerized form.

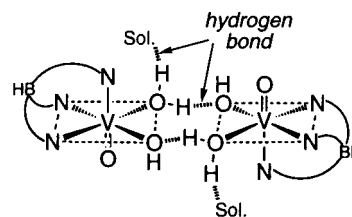
Elemental analysis suggested that a composition of **4** was a hydroxo-aqua complex formulated as Tp^{Pr₂}V(O)(OH)(OH₂).

The structure of **4** was finally confirmed by X-ray crystallography (Figure 3 and Table 4). A six-coordinate octahedral VO²⁺ center is supported by a tridentate κ³-Tp^{Pr₂} ligand as found for **1** and **2**; a nitrogen donor (N11) sitting trans to the oxo ligand is at a distance of 2.346(3) Å from the vanadium center, and the remaining two nitrogen atoms form the basal plane of the octahedron. The most striking structural feature is dimerization of two monomeric units via hydrogen bonds between the hydroxide and aqua ligands resulting in H₃O₂⁻ bridging ligands, as is evidenced by the short O...O distance (2.441(1) Å) (Chart 2). The distinguishable two V–O bond lengths of 1.970(3) and 2.020(3) Å indicate that they are assigned to the hydroxo and aqua parts of H₃O₂⁻, respectively.^{20,21} The distance between two vanadium centers is 5.184(1) Å, and the V=O moieties are located in an *anti*-configuration. In addition, the remaining aqua hydrogen atoms interact weakly with Et₂O as

Table 4. Selected Bond Lengths (Å) and Bond Angles (deg) for 4·2Et₂O

Bond Lengths					
V1–O1	1.588(2)	V1–O2	1.970(3)	V1–O3	2.020(3)
V1–N11	2.346(3)	V1–N21	2.115(3)	V1–N31	2.125(3)
O2–H1	0.68(4)	O3–H2	1.15(4)	O3–H3	0.62(4)
O2–H2'	1.35(4)	O2...O3'	2.441(4)	V1...V1'	5.184(1)
Bond Angles					
O1–V1–O2	100.1(1)	O1–V1–O3	99.7(1)		
O1–V1–N11	174.4(1)	O1–V1–N21	94.9(1)		
O1–V1–N31	94.7(1)	O2–V1–O3	88.4(1)		
O2–V1–N11	84.2(1)	O2–V1–N21	91.0(1)		
O2–V1–N31	165.1(1)	O3–V1–N11	83.9(1)		
O3–V1–N21	165.3(1)	O3–V1–N31	89.5(1)		
N11–V1–N21	81.4(1)	N11–V1–N31	81.0(1)		
N21–V1–N31	87.2(1)	V1–O2–H1	117(4)		
V1–O3–H2	112(1)	V1–O3–H3	118(4)		
H2–O3–H3	124(4)				

Chart 2



indicated by an O...O distance of 2.9 Å.²² In conclusion, **4** is alternatively formulated as [Tp^{Pr₂}V(O)(μ-H₃O₂⁻)]₂. Although some hydroxo-aqua (or μ-H₃O₂⁻) complexes had been known to give corresponding dehydrated μ-hydroxo complexes via loss of an aqua ligand by heating under vacuum,^{20d} no dehydrated dinuclear complex, [Tp^{Pr₂}V(O)(μ-OH)]₂, was obtained from **4**. It is worth noting that the dimeric structure bridged by the μ-H₃O₂⁻ ligand is held in solution as is evidenced by its IR spectrum of a CH₂Cl₂ solution, containing two ν(O–H) bands at 3676 and 3620 cm⁻¹.

As we indicated above, the treatment of the chloro complexes with the aqueous NaOH caused partial decomposition of the chloro complexes, and heating of the resultant reaction mixture (obtained by removal of the water layer followed by evaporation of the solvent) gave another hydroxo complex **5**, which had a trinuclear VO²⁺ bis(μ-hydroxo)bis(μ-pyrazolato) structure. In

- (20) (a) Bino, A.; Gibson, D. *Inorg. Chem.* **1984**, *23*, 109. (b) Ardon, M.; Bino, A. *Inorg. Chem.* **1985**, *24*, 1343. (c) Galasbøl, F.; Larsen, S.; Rasmussen, B.; Springborg, J. *Inorg. Chem.* **1986**, *25*, 290. (d) Ardon, M.; Bino, A.; Michelsen, K. *J. Am. Chem. Soc.* **1987**, *109*, 1986. (e) Bossek, U.; Wieghardt, K.; Nuber, B.; Weiss, J. *Angew. Chem., Int. Ed. Engl.* **1990**, *29*, 1055. (f) Schneider, R.; Weyhermüller, T.; Wieghardt, K.; Nuber, B. *Inorg. Chem.* **1993**, *32*, 4925. (g) Hazell, A.; Jensen, K. B.; McKenzie, C. J.; Toftlund, H. *Inorg. Chem.* **1994**, *33*, 3127. (h) Dong, Y.; Fujii, H.; Hendrich, M. P.; Leising, R. A.; Pan, G.; Randall, C. R.; Wilkinson, E. C.; Zang, Y.; Que, L., Jr.; Fox, B. G.; Kauffmann, K.; Münck, E. *J. Am. Chem. Soc.* **1995**, *117*, 2778. (i) Ruf, M.; Weis, K.; Vahrenkamp, H. *J. Am. Chem. Soc.* **1996**, *118*, 9288. (j) Knopp, P.; Wieghardt, K.; Nuber, B.; Weiss, J.; Sheldrick, W. S. *Inorg. Chem.* **1990**, *29*, 363. (k) Jüstel, T.; Bendix, J.; Metzler-Nolte, N.; Weyhermüller, T.; Nuber, B.; Wieghardt, K. *Inorg. Chem.* **1998**, *37*, 35. (l) Meyer, F.; Rutsch, P. *Chem. Commun.* **1998**, 1037. (m) Poussereau, S.; Blondin, G.; Cesario, M.; Guilhem, J.; Chottard, G.; Gonnet, F.; Girerd, J.-J. *Inorg. Chem.* **1998**, *37*, 3127. (21) Formation of the intermolecular hydrogen bonds (except the μ-H₃O₂⁻ structure) in vanadium complexes were observed in the following reports: (a) Vergopoulos, V.; Prietsch, W.; Fritzsche, M.; Rehder, D. *Inorg. Chem.* **1993**, *32*, 1844. (b) Crans, D. C.; Mahroof-Tahir, M.; Anderson, O. P.; Miller, M. M. *Inorg. Chem.* **1994**, *33*, 5586. (22) The intermolecular hydrogen bonding networks between the metal-coordinating H₂O ligands and the solvent or counteranion molecules are observed in the Ru complexes with the same Tp^{Pr₂} ligand. See ref 4d.

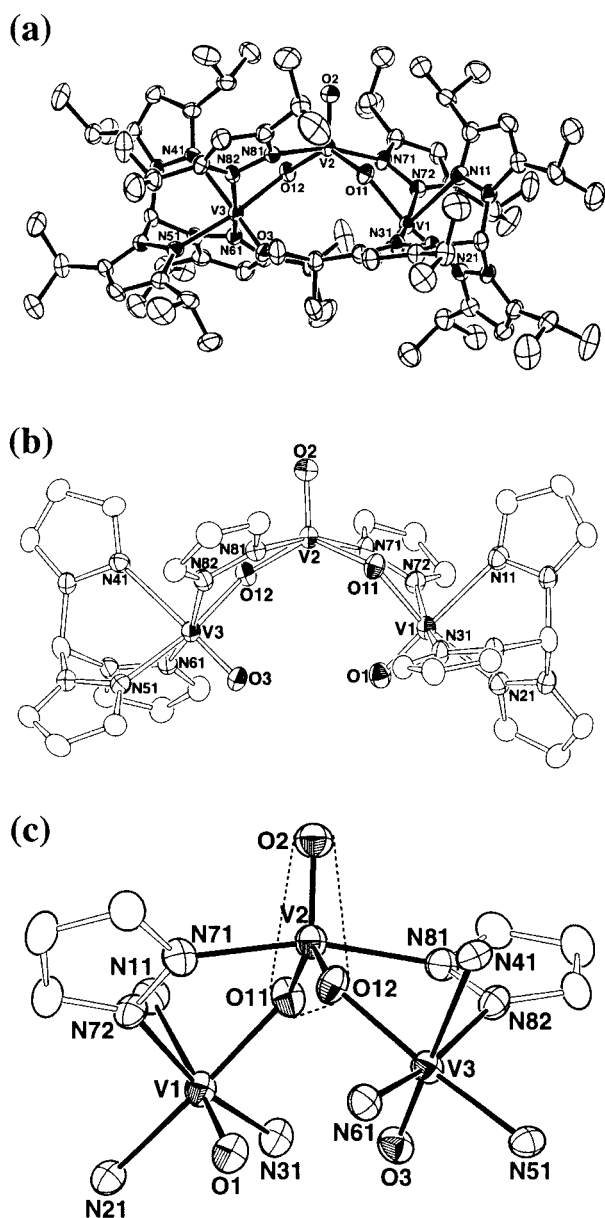


Figure 4. ORTEP drawing of $\text{Tp}^{\text{Pr}_2}\text{V}(\text{O})(\mu\text{-OH})(\mu\text{-Pz}^{\text{Pr}_2})\text{V}(\text{O})(\mu\text{-OH})(\mu\text{-Pz}^{\text{Pr}_2})\text{V}(\text{O})\text{Tp}^{\text{Pr}_2}\cdot 2\text{Et}_2\text{O}$ (**5**· $2\text{Et}_2\text{O}$) (drawn at the 50% probability level). (a) Whole molecule of **5**. All hydrogen atoms and the Et_2O molecules are omitted for clarity. (b) All isopropyl groups on the Tp^{Pr_2} and bridging Pz^{Pr_2} ligands are omitted for clarity. (c) Expanded view of the trinuclear metal centers.

its IR spectrum, only a single $\nu(\text{O}-\text{H})$ band at 3630 cm^{-1} was clearly distinguishable from that of **4**, and the two $\text{V}=\text{O}$ vibrations at 981 and 975 cm^{-1} indicated the presence of electronically different VO^{2+} units.

X-ray crystallographic analysis revealed that the trinuclear hydroxo complex **5** consists of two $\text{Tp}^{\text{Pr}_2}\text{V}(\text{O})$ fragments (V1 and V3) and VO^{2+} (V2) only supported by two sets of hydroxo and pyrazolato ligands and has a pseudo C_2 symmetry along the $\text{V2}-\text{O2}$ axis and bisecting the angle $\text{O11}-\text{V2}-\text{O12}$ (Figure 4 and Table 5). The $\text{Tp}^{\text{Pr}_2}\text{V}$ centers (V1 and V3) take an octahedral geometry coordinated by an N_4O_2 donor set, and the geometry of V2 is a trigonal bipyramid, consisting of the $\text{N71}-\text{V2}-\text{N81}$ axis and the $\text{O1}-\text{O11}-\text{O12}$ basal plane (see part c of Figure 4), as is evidenced by the nearly linear angle of $\text{N}-\text{V}-\text{N}$ (163.7°) and the sum of the $\text{O}-\text{V}-\text{O}$ angles ($\text{O2}-\text{V2}-\text{O11}$, 112.7° ; $\text{O2}-\text{V2}-\text{O12}$, 114.0° ; $\text{O11}-\text{V2}-\text{O12}$, 133.2° ; total = 359.9°). Each of the $\text{Tp}^{\text{Pr}_2}\text{V}(\text{O})$ fragments and the central

Table 5. Selected Bond Lengths (\AA) and Bond Angles (deg) for **5**· $2\text{Et}_2\text{O}$

Bond Lengths			
V1—O1	1.589(3)	V1—O11	2.003(2)
V1—N21	2.153(3)	V1—N31	2.101(4)
V2—O2	1.591(3)	V2—O11	1.934(3)
V2—N71	2.099(3)	V2—N81	2.097(4)
V3—O12	2.020(3)	V3—N41	2.362(3)
V3—N61	2.113(3)	V3—N82	2.118(3)
V2...V3	3.4949(9)	V1...V3	5.4585(8)
V1—N11	2.389(3)	V1—N72	2.106(4)
V2—O12	1.945(2)	V3—O3	1.591(3)
V3—N51	2.127(4)	V1...V2	3.444(1)

Bond Angles			
O1—V1—O11	100.4(1)	O1—V1—N11	177.9(1)
O1—V1—N21	93.7(1)	O1—V1—N31	97.7(1)
O1—V1—N72	93.9(1)	O11—V1—N11	81.7(1)
O11—V1—N21	163.2(1)	O11—V1—N31	86.4(1)
O11—V1—N72	83.5(1)	N11—V1—N21	84.3(1)
N11—V1—N31	82.5(1)	N11—V1—N72	86.2(1)
N21—V1—N31	82.6(1)	N21—V1—N72	104.8(1)
N31—V1—N72	165.9(1)	O2—V2—O11	112.7(1)
O2—V2—O12	114.0(1)	O2—V2—N71	98.7(2)
O2—V2—N81	97.5(1)	O11—V2—O12	133.2(1)
O11—V2—N71	82.4(1)	O11—V2—N81	90.2(1)
O12—V2—N71	91.2(1)	O12—V2—N81	83.3(1)
N71—V2—N81	163.7(1)	O3—V3—O12	97.8(1)
O3—V3—N41	177.6(1)	O3—V3—N51	92.0(1)
O3—V3—N61	97.7(1)	O3—V3—N82	96.4(1)
O12—V3—N41	83.6(1)	O12—V3—N51	168.5(1)
O12—V3—N61	90.8(1)	O12—V3—N82	84.0(1)
N41—V3—N51	86.5(1)	N41—V3—N61	80.4(1)
N41—V3—N82	85.6(1)	N51—V3—N61	82.0(1)
N51—V3—N82	100.9(1)	N61—V3—N82	165.5(1)
V1—O11—V2	122.0(1)	V2—O12—V3	123.6(1)

VO^{2+} unit are bridged by the hydroxo and pyrazolato ligands, and the adjacent $\text{V}=\text{O}$ moieties are arranged in an *anti*-configuration. Such a (μ -hydroxo)(μ -pyrazolato)-bridging structure has been also observed for the dinuclear $\text{Mn}(\text{II})$ complex with the same Tp^{Pr_2} ligand.²³

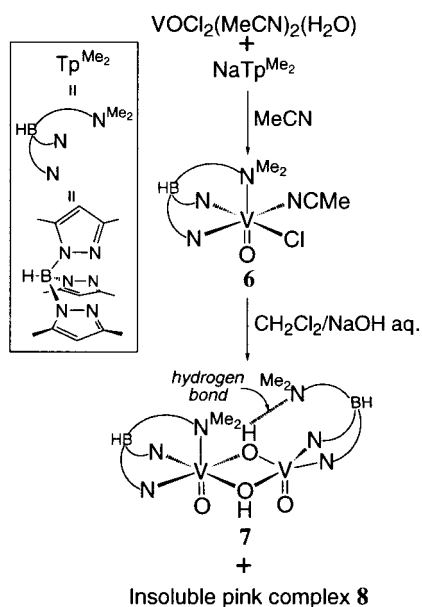
It is worth noting that **5** is formed by the heating of the crude reaction mixture that consists of **4** and an H_2O -insoluble vanadium compound coordinated by Pz^{Pr_2} (pyrazolate anion) or/and $\text{Pz}^{\text{Pr}_2}\text{H}$ (neutral pyrazole) ligands,²⁴ arising from the partial decomposition of the chloro complexes, although the treatment of the reaction mixture without heating resulted in isolation of **4**. In addition, heating of the highly pure isolated **4** in the presence of $\text{Pz}^{\text{Pr}_2}\text{H}$ and $\text{VOCl}_2(\text{MeCN})_2(\text{H}_2\text{O})$ did not yield **5**. We thus conclude that the bridging pyrazolate ligands and the non- Tp^{Pr_2} -supported vanadium center come from the $\text{VO}^{2+}-\text{Pz}^{\text{Pr}_2}$ ($\text{Pz}^{\text{Pr}_2}\text{H}$) compound formed under basic conditions (i.e., treatment of the chloro complex with the aqueous NaOH), and thermal coupling of **4** and the VO^{2+} -pyrazolato compound results in formation of **5** concomitant with dehydration from **4**, although the OH-bridged dinuclear complex, $[\text{Tp}^{\text{Pr}_2}\text{V}(\text{O})(\mu\text{-OH})_2]$, does not form in any conditions (vide supra).

2. Synthesis of Tp^{Me_2} Complexes. Although the chloro complexes with Tp^{Me_2} have been prepared, no corresponding hydroxo complex is reported so far. In this study, a hydroxo

(23) Komatsuzaki, H.; Ichikawa, S.; Hikichi, S.; Akita, M.; Moro-oka, Y. *Inorg. Chem.* **1998**, *37*, 3652.

(24) The heterogeneous two-layer reaction system (i.e., the reaction of the toluene solution of the chloro complex with aqueous NaOH) would afford removal of a water-soluble compound (such as metal salts) from the crude product upon the separation of two layers. In this study, therefore, a non- Tp -supported vanadium compound must be a H_2O -insoluble compound, and the pyrazolato (or pyrazole) complex formed by coordination of the alkyl-substituted pyrazolyl and/or neutral pyrazole (i.e., Pz^{Pr_2-} and/or $\text{Pz}^{\text{Pr}_2}\text{H}$) to a VO^{2+} center might be soluble not to H_2O but to the toluene layer. Further characterization of the resulting toluene-layer-soluble VO^{2+} compound (i.e., $\text{VO}^{2+}-\text{Pz}^{\text{Pr}_2}$ complex) was not performed.

Scheme 2



complex **7** with the less hindered Tp^{Me₂} ligand was also prepared and characterized. In addition, a novel chloro complex with Tp^{Me₂} **6** is synthesized (Scheme 2).

(a) Chloro Complex 6. The previously reported VO²⁺–chloro complex with Tp^{Me₂} involved the additional pyrazole ligand, arising from the decomposed Tp^{Me₂} moiety.^{10b} In the present study, we modified the reaction condition originally reported by Collison et al.; NaTp^{Me₂} was used instead of KTp^{Me₂}. Preparation of a pure sample of the sodium salt of Tp^{Me₂} was easier than that of the potassium salt, although the original report described that the presence of the pyrazole ligand did not affect the formation of Tp^{Me₂}V(O)Cl(Pz^{Me₂}H).^{10b} As a result, we succeeded in getting an MeCN-incorporated chloro complex, Tp^{Me₂}V(O)Cl(NCMe) (**6**), instead of the Pz^{Me₂}H adduct, in a reasonable yield. An IR spectrum of the blue solid of **6** contained peaks around 2250–2315 cm⁻¹, which were attributed to C≡N vibration of the coordinating MeCN molecule. The molecular structure of **6** was confirmed by X-ray crystallography as presented in Figure 1 and Table 2.

Although the structure of the solid state of **6** was similar to the other Tp^RV(O)Cl(X) complexes (vide infra), dissociation of the neutral supporting ligand MeCN was observed in the solution state. A MeCN solution of **6** showed a blue color as found for the other chloro complexes; however, dissolving of the blue solid of **6** in toluene gave a pale brownish yellow solution. In contrast, no significant color change was observed for the Tp^{Pr₂} complexes containing Pz^{Pr₂}H (**1**) and pyridine (**2**) when they dissolved in noncoordinating solvents, such as CH₂Cl₂ and toluene. ESR spectra of the obtained chloro complexes might also reflect the dissociation behavior of the MeCN ligand of **6**. Relatively sharp spectral features of the toluene glass of **1** and **2** resembled that of the previously reported Tp^{Me₂}V(O)Cl(Pz^{Me₂}H),^{10b} but the MeCN adduct **6** showed broad absorption patterns for the frozen glass of any solvents, including MeCN (Figure 2 in the Supporting Information).

When NaTp^{Me₂} was allowed to react with VOCl₂ instead of VOCl₂(MeCN)₂(H₂O), the Tp^{Me₂} moiety was partially decomposed to give the pyrazole-containing complex, Tp^{Me₂}V(O)Cl(Pz^{Me₂}H),^{10b} in a relatively low yield. Coordination of the neutral pyrazole ligand was confirmed by its IR spectrum, which contained a ν(N–H) absorption of the coordinating pyrazole at 3306 cm⁻¹ 2d.e.19 and a FD-MS spectrum (*m/z* = 496, M⁺). It is

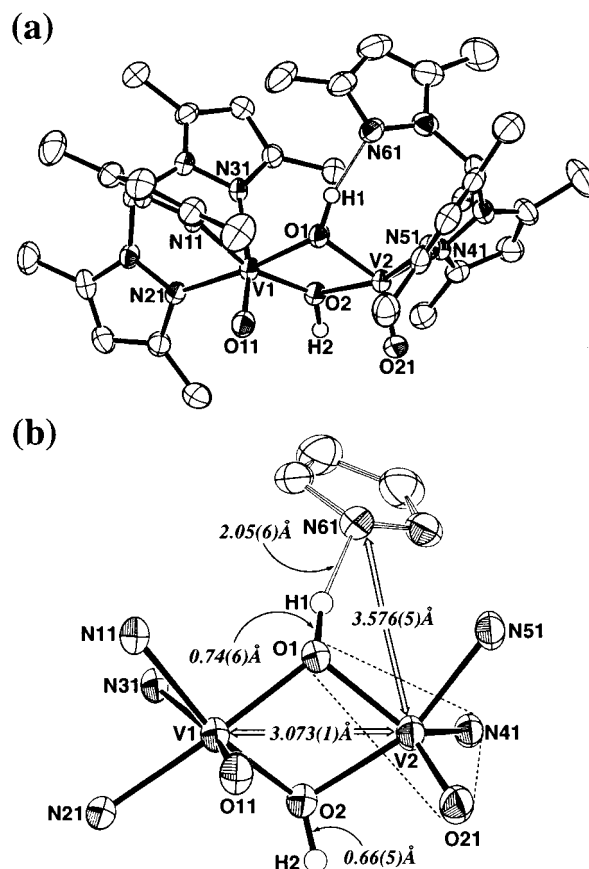


Figure 5. ORTEP drawing of (κ^3 -Tp^{Me₂})V(O)(μ -OH)₂V(O)(κ^2 -Tp^{Me₂})·CH₂Cl₂ (**7**·CH₂Cl₂) (drawn at the 50% probability level). (a) Whole molecule of **7**. All hydrogen atoms except those attached to the oxygen atoms of the hydroxo ligands and the CH₂Cl₂ molecule are omitted for clarity. (b) Expanded view of the metal centers, including the non-metal-coordinating pyrazolyl group in the κ^2 -Tp^{Me₂} ligand.

notable that no MeCN adduct **6** was obtained, although the reaction was carried out in MeCN solvent. These observations imply that the composition and the yield of the products may be governed by a mix of vanadium compounds and the counterions of Tp^{Me₂}.

(b) Hydroxo Complexes 7 and 8. Hydrolysis of **6** by an aqueous NaOH solution resulted in yielding two different hydroxo complexes, depending on reaction solvents. A heterogeneous reaction of a CH₂Cl₂ solution of **6** and the aqueous NaOH solution gave a bluish purple solution **7** and a small amount of a pink precipitate **8**. Appropriate workup of the CH₂Cl₂ layer afforded a bluish purple crystalline solid of a hydroxo complex **7**. A sharp peak of ν(O–H) appeared at 3635 cm⁻¹ in its IR spectrum, and its unique unsymmetrical dinuclear structure was revealed by X-ray crystallography (Figure 5 and Table 6).

The bluish purple complex **7** has a dinuclear bis(μ -hydroxo) structure, which consists of two structurally different metal centers. One metal center (V1) has an octahedral geometry coordinated by a N₃O₃ donor set, coming from three nitrogen atoms of a tridentate κ^3 -Tp^{Me₂} moiety, a terminal oxo ligand, and two bridging hydroxide ligands. In contrast, a geometry of the other vanadium center (V2) is best described as a distorted trigonal bipyramid composed from the O21 (terminal oxide)–O1 (bridging hydroxide)–N41 (pyrazolyl) trigonal basal plane and the O2 (hydroxide)–N51 (pyrazolyl) axis. In the V2 center, Tp^{Me₂} is not coordinating to the metal center with a tridentate (κ^3) but a bidentate (κ^2) mode. The distance of 3.576(5) Å between V2 and the noncoordinating pyrazolyl nitrogen (N61)

Table 6. Selected Bond Lengths (Å) and Bond Angles (deg) for 7·CH₂Cl₂

Bond Lengths					
V1–O1	1.977(4)	V1–O2	2.018(4)	V1–O11	1.607(4)
V1–N11	2.119(4)	V1–N21	2.127(4)	V1–N31	2.369(4)
V2–O1	1.934(4)	V2–O2	2.027(4)	V2–O21	1.597(4)
V2–N41	2.046(4)	V2–N51	2.099(5)	V2···N61	3.576(5)
O1–H1	0.74(6)	O2–H2	0.66(5)	O1···N61	2.750(6)
V1···V2	3.073(1)				
Bond Angles					
O1–V1–O2	75.2(2)	O1–V1–O11	98.0(2)		
O1–V1–N11	92.2(2)	O1–V1–N21	170.3(2)		
O1–V1–N31	92.4(2)	O2–V1–O11	100.3(2)		
O2–V1–N11	162.5(2)	O2–V1–N21	102.1(1)		
O2–V1–N31	86.6(2)	O11–V1–N11	93.4(2)		
O11–V1–N21	91.7(2)	O11–V1–N31	168.7(2)		
N11–V1–N21	88.2(2)	N11–V1–N31	81.8(2)		
N21–V1–N31	78.0(2)	O1–V2–O2	75.9(2)		
O1–V2–O21	127.7(2)	O1–V2–N41	122.9(2)		
O1–V2–N51	84.2(2)	O2–V2–O21	168.3(2)		
O2–V2–N41	98.9(2)	O2–V2–N51	159.9(2)		
O21–V2–N41	109.4(2)	O21–V2–N51	96.1(2)		
N41–V2–N51	89.4(2)	V1–O1–V2	103.6(2)		
V1–O2–V2	98.8(2)	V1–O1–H1	120(5)		
V2–O1–H1	113(5)	V1–O2–H2	126(5)		
V2–O2–H2	114(5)	O1–H1···N61	157(6)		

indicates no interaction between them; however, it interacts with one of the two bridging hydroxo ligands (O1) via hydrogen bond (O1···N61, 2.750(6) Å; O1–H1, 0.74(6) Å; H1–N61, 2.05(6) Å; O1–H1–N61, 157(6)°). The most striking structural feature is that two V=O units are located in a *syn*-configuration with the dihedral angle of O11–V1–V2–O21 = 24.9°; on the other hand, the previously reported dinuclear VO²⁺ bis(*μ*-hydroxo) complexes with Tp^{H₂} or 1,4,7-triazacyclononane²⁵ have the crystallographically imposed inversion centers, resulting in an *anti*-configuration of the two V=O units.

The unique unsymmetrical environment of the metal centers of **7** was also suggested by a broad $\nu(\text{B-H})$ band around 2520 cm⁻¹ and two distinguishable $\nu(\text{V=O})$ bands at 981 and 958 cm⁻¹ in its solid-state IR spectrum. In addition to the sharp $\nu(\text{O-H})$ peak at 3635 cm⁻¹, the broad peak was observed around 3539 cm⁻¹ for the solid sample, supporting the presence of the hydrogen-bonded OH group. An IR spectrum of a CH₂-Cl₂ solution contained two sets of $\nu(\text{B-H})$ (2545 and 2527 cm⁻¹) and $\nu(\text{V=O})$ (983 and 953 cm⁻¹) vibrations, although only a single sharp peak was observed at 3629 cm⁻¹ and the broad band attributed to the hydrogen-bonded OH group disappeared. Existence of the two sets of $\nu(\text{B-H})$ and $\nu(\text{V=O})$ may imply that the dinuclear vanadium species still have an unsymmetrical structure. Especially, the $\nu(\text{B-H})$ peaks in both the solid and solution states were observed above 2500 cm⁻¹ in the range of the $\nu(\text{B-H})$ value, typical for the κ^3 -binding Tp^R ligand.²⁶ As indicated above, the non-metal-supporting nitrogen atom in the κ^2 -Tp^{Me₂} interacted with the OH group, and therefore, the $\nu(\text{B-H})$ band attributed to the κ^2 -Tp^{Me₂} in **7** was expected to appear in the region similar to that of the κ^3 -Tp^{Me₂} ligand. On the basis of these observations, we conclude that **7** keeps the unsymmetrical structure in the solution²⁷ and the absence of the broad $\nu(\text{O-H})$ band is due to the strong hydrogen-bonding interaction between one of the two bridging

hydroxo groups and the nitrogen atoms in κ^2 -Tp^{Me₂} in the solution state.²⁸

The pink precipitate **8** also contained an IR absorption band of the $\nu(\text{B-H})$ at 2515 cm⁻¹. One possible assignment for **8** is a monomeric hydroxo-aqua (or a dimeric bis(*μ*-H₃O₂⁻)) complex that is similar to the Tp^{Pr₂} derivative **4** (vide supra) because (1) the IR spectral features of **8** (existence of two $\nu(\text{O-H})$ at 3657 and 3603 cm⁻¹ and a single $\nu(\text{V=O})$ at 979 cm⁻¹) are similar to those of **4**, (2) the result of an elemental analysis is consistent with the composition of the hydroxo-aqua complex, and (3) heating of a solid sample of **8** under vacuum gives the non-H₂O-containing complex **7**.^{20d} However, **8** could not be further characterized because of its insolubility in any organic solvents. It is notable that only **8** has been obtained by treatment of MeCN or toluene solutions of **6** with the aqueous NaOH.

3. An Attempt to Prepare a Tp^{Bu^t,Prⁱ} Complex. We also attempted to prepare VO²⁺ complexes with the more sterically demanding Tp^{Bu^t,Prⁱ} ligand, but any Tp^{Bu^t,Prⁱ}V(O) compound was not obtained. Our previous studies about the Fe complexes have indicated that the formation of a six-coordinate octahedral metal complex with the Tp^{Bu^t,Prⁱ} ligand is impossible, although the five-coordinate trigonal-bipyramidal Fe complexes are obtained.^{2e,29} We expected to form a five-coordinate trigonal-bipyramidal V(IV) complex with a formulation as Tp^{Bu^t,Prⁱ}V(O)Cl because some *tbp* VO²⁺ compounds were known.¹⁷ However, reactions of Tp^{Bu^t,Prⁱ} with the VO²⁺ compounds (VOCl₂(MeCN)₂(H₂O) and VOCl₂) resulted in perfect decomposition of Tp^{Bu^t,Prⁱ}, although the B–N bonds of which were in the hydrophobic shading pocket formed by three 5-isopropyl groups. As we described above, partial decomposition of the Tp^{Pr₂} moiety occurred during the metathesis of M'Tp^{Pr₂} (M' = K or Na) with VOCl₂(MeCN)₂(H₂O), although not the Pz^{Me₂}-H but the MeCN adduct was obtained when NaTp^{Me₂} reacted with VOCl₂(MeCN)₂(H₂O). We thus conclude that steric hindrance of the *tert*-butyl substituents accelerates the decomposition of Tp^{Bu^t,Prⁱ}.

4. Structural Comparison of the Tp^RV(O) Complexes. All the chloro complexes, including the previously reported Tp^{Me₂} derivatives Tp^{Me₂}V(O)Cl(DMF)^{10a} and Tp^{Me₂}V(O)Cl(Pz^{Me₂}H),^{10b} have almost the identical structure irrespective of the supporting Tp^R ligands, whereas the hydroxo complexes exhibit four different structures (including the previously reported dinuclear structure with Tp^{H₂}), depending on the supporting Tp^R ligands. In this section, we discuss about the relation between the steric hindrance of Tp^R and the solid-state structures revealed by X-ray crystallography.

(27) Another possible explanation for the appearance of two sets of the $\nu(\text{B-H})$ and $\nu(\text{V=O})$ is existence of a fast equilibrium between the dimer and monomer of Tp^{Me₂}V(O)(OH) in the solution. ¹H NMR spectrum of **7** gave broad paramagnetically shifted signals in the 1–16 ppm region, although the Tp^{Pr₂} derivative **4**, which involved the relatively long distant (5.18 Å) two vanadium centers, showed very broad absorptions arising from impurities in the 1–7 ppm region (Figure 4 in the Supporting Information). In the low-temperature ESR spectra, both **7** and **4** (toluene glass) showed complicated features due to coupling of the vanadium nucleus spins (Figure 3 in the Supporting Information). In sum, we could not exclude the possibilities of the fast equilibrium or structural change for the solution state of **7**.

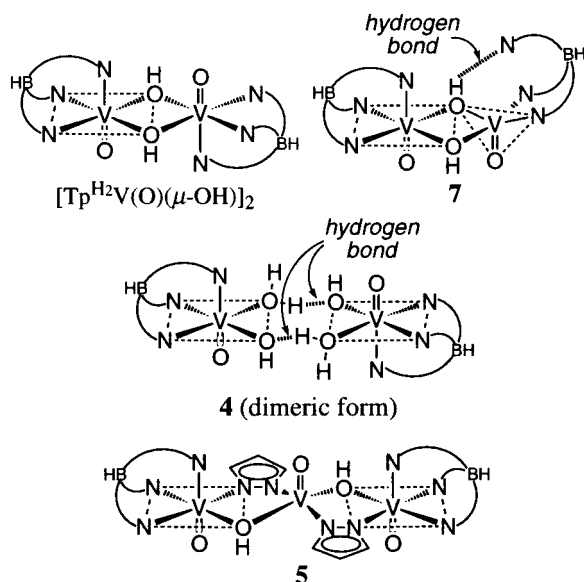
(28) Formation of the hydrogen bond results in broadening of the absorption of the vibration between the hydrogen and its binding atoms, and if the hydrogen bonding interaction becomes stronger, the corresponding vibration will be concealed from the spectrum. For example, strong hydrogen bonding interaction between the metal-coordinating pyrazole's NH and the carboxylate oxygen atom results in the absence of the $\nu(\text{N-H})$ band. See refs 2e, 10b, 19, and Kitajima, N.; Osawa, M.; Tamura, N.; Moro-oka, Y.; Hirano, T.; Hirobe, M.; Nagano, T. *Inorg. Chem.* **1993**, *32*, 1879.

(29) Ogihara, T.; Hikichi, S.; Akita, M.; Moro-oka, Y. *Inorg. Chem.* **1998**, *37*, 2614.

(25) Wieghardt, K.; Bossek, U.; Volckmar, K.; Swiridoff, W.; Weiss, J. *Inorg. Chem.* **1984**, *23*, 1387. A *syn*-arranged VO²⁺-containing hydroxo complex with a dinucleating ligand has been reported. Neves, A.; Wieghardt, K.; Nuber, B.; Weiss, J. *Inorg. Chim. Acta* **1988**, *150*, 183.

(26) Dependence of the $\nu(\text{B-H})$ values on the hapticity of the Tp^{Pr₂} ligand is observed. See ref 4f.

Chart 3

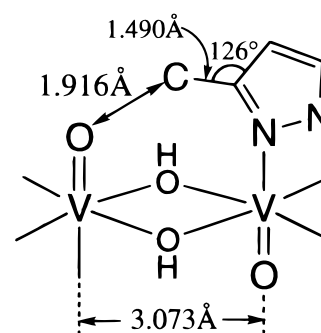


(a) **Chloro and Acetylacetonato Complexes.** In Figure 1, molecular structures of the chloro complexes of the Tp^{Pr₂} derivatives **1** and **2**, and the MeCN-containing Tp^{Me₂} derivative **6** obtained in this study, are presented. The bond lengths and angles for the metal centers of Tp^RV(O)(Cl)(X) (including the previously reported DMF or Pz^{Me₂}H containing Tp^{Me₂} complexes¹⁰) are summarized in Table 2. No specific structural feature depending on the Tp^R ligands is observed. Although the V=O vibrations of a series of the chloro complexes depend on the Tp^R ligands in IR spectra (**1**, 977 cm⁻¹; **2**, 975 cm⁻¹; **6**, 966 cm⁻¹; Tp^{Me₂}V(O)Cl(DMF), 965 cm⁻¹; Tp^{Me₂}V(O)Cl-(Pz^{Me₂}H), 964 cm⁻¹), the bond lengths of V=O are not correlated with their vibration values.

In the case of the acetylacetonato complexes, overall structure of the Tp^{Pr₂} complex **3** is analogous to that of the Tp^{Me₂} derivative (reported in ref 11), although the distances between the vanadium center and the N₂O₂ donors constituting the basal plane of the octahedron (i.e. V–O and V–N_{eq}) in **3** are shorter than those of the Tp^{Me₂} complex, and the order of the V=O lengths is inverse (i.e., **3** > Tp^{Me₂}V(O)(acac)) because of the Jahn–Teller distortion (Table 3). In conclusion, the structures of the six-coordinate mononuclear complexes containing the same anionic ligands (i.e., Cl⁻ or acac⁻) show no Tp^R-depending structural features.

(b) **Hydroxo Complexes.** Schematic drawings of the structurally characterized hydroxo complexes are presented in Chart 3. In the previously reported vanadyl (VO²⁺) hydroxo complex with Tp^{H₂}, the dinuclear V(IV) centers are bridged solely by two hydroxo groups, as found in Tp^{Pr₂}M(μ-OH)₂MTp^{Pr₂} (M = Mn to Cu),^{2a–d} although the two V(IV) centers separated by 3.122 Å are 6-coordinated by N₃O₃ ligand donor sets, and the two V=O units are arranged in *anti*-fashion.⁸ In contrast, the present Tp^{Me₂} derivative **7** has the unsymmetrical dinuclear bis-(μ-hydroxo) structure consisting of the *syn*-arranged V=O moieties (distance of V···V = 3.073 Å). It is notable that the dinuclear bis-(μ-hydroxo) complex of Cu(II) with the Tp^{Me₂} ligand has a symmetrical, dimeric structure that sits on a crystallographically imposed inversion center (Cu···Cu separation is 3.059 Å), although the coordination numbers of the metal centers are five.³⁰ Because of the steric repulsion between the

Chart 4



substituents at the pyrazolyl 3-positions on the two facing Tp^R ligands, an *anti*-configuration may be favorable. In the case of the Tp^{Me₂} complex **7**, however, steric hindrance between the terminal oxo ligand and one of the three 3-methyl substituents on Tp^{Me₂} that supports the other vanadium center may make the *anti*-configuration unstable to result in the highly unsymmetrical dinuclear structure of **7**. In fact, we examined a symmetrical dinuclear bis-(μ-hydroxo) structure obtained by superimposing 3-methyl substituents on the pyrazolyl groups of [Tp^{H₂}V(O)(μ-OH)]₂,⁸ a distance between the oxo ligand and the imposed carbon atom, which was the substituent of the pyrazolyl group sitting at *trans* to the other terminal oxo ligand, was only 1.916 Å (Chart 4, Figure 5 in the Supporting Information).

In the Tp^{Pr₂} system, a dinuclear bis-(μ-hydroxo) complex like the Tp^{H₂} and Tp^{Me₂} derivatives is not obtained, although the dimerized hydroxo–aqua complex **4** and the trinuclear bis-(μ-hydroxo)–bis-(μ-pyrazolato) complex **5** are isolated. These observations may imply that a hydroxo ligand favors a bridging coordination mode arising from a lone pair on their oxygen atoms, but steric hindrance of the Prⁱ groups on Tp^{Pr₂} makes formation of a bis-(μ-hydroxo) dinuclear VO²⁺ core with a face-to-face orientation of two Tp^{Pr₂} moieties impossible.

Concluding Remarks

Novel VO²⁺ chloro and hydroxo complexes with the sterically demanding Tp^{Pr₂} and Tp^{Me₂} ligands were prepared and structurally characterized, although the more hindered Tp^{Buⁱ,Prⁱ} ligand could not yield the desired Tp^{Buⁱ,Prⁱ}V(O) complex.

Ligand displacement of VOCl₂(MeCN)₂(H₂O) by Tp^{Pr₂} resulted in formation of the octahedral chloro complexes, containing the pyrazole or pyridine ligands, Tp^RV(O)(Cl)(X) (**1**, X = Pz^{Pr₂}H; **2**, X = py), although the partial decomposition of Tp^{Pr₂} occurred under any reaction conditions. Hydrolysis of the obtained chloro complexes afforded the hydroxo complexes. In the hydroxo–aqua complex **4**, the intermolecular hydrogen-bonding interaction between the hydroxo and the aqua ligands resulted in dimerization of the Tp^{Pr₂}V(O) fragments bridged by H₃O⁺. The trinuclear complex **5** is formed via coupling of the hydroxo–aqua complex **4** and the VO²⁺–pyrazolato compound resulting from the partial decomposition of the chloro complexes during the hydrolysis. The trinuclear core consists of two octahedral Tp^{Pr₂}V(O) fragments and the distorted trigonal bipyramidal non-Tp^{Pr₂}-supported vanadium center sitting on the pseudo C₂ symmetry axis.

The MeCN-containing chloro complex with the Tp^{Me₂} ligand, Tp^{Me₂}V(O)(Cl)(NCMe) (**6**), instead of the previously reported Pz^{Me₂}H adduct, was obtained by the reaction of NaTp^{Me₂} with VOCl₂(MeCN)₂(H₂O) in relatively high yield. Hydrolysis of **6** yielded the dinuclear bis-(μ-hydroxo) complex with Tp^{Me₂} (**7**),

(30) Kitajima, N.; Koda, T.; Hashimoto, S.; Kitagawa, T.; Moro-oka, Y. *J. Am. Chem. Soc.* **1991**, *113*, 5664.

which consisted of the *syn*-arranged V=O fragments having the different coordination geometries (octahedron with κ^3 -Tp^{Me₂} and trigonal bipyramid with κ^2 -Tp^{Me₂}) of the vanadium centers. Intramolecular hydrogen-bonding interaction between one of the two hydroxide ligands and the non-metal-supporting pyrazolyl nitrogen atom in κ^2 -Tp^{Me₂} was observed.

The difference of the steric hindrance of the alkyl substituents on Tp^R led to the considerably different secondary structures of the hydroxo complexes, although the coordination environment of the vanadium centers of the six-coordinate mononuclear chloro or acetylacetonato complexes were essentially identical.

(31) The hydroxo complexes of **4** and **7** react with various protic acids (such as carboxylic acids and phenols) to give the corresponding V^{IV}-(O) complexes via dehydrative condensation. Also, they are oxygenated by H₂O₂ and O₂ to give novel dioxygen complexes.

Investigations of reactivities of the obtained hydroxo complexes are now in progress, and the results will be reported in due course.³¹

Acknowledgment. This research was supported in part by a Grant-in-Aid for Specially Promoted Scientific Research (No. 08102006) from the Ministry of Education, Science, Sports and Culture of the Japanese government.

Supporting Information Available: Atomic coordinates, thermal parameters, interatomic distances, and bond angles for **1**, **2**·Et₂O, **3**, **4**·2Et₂O, **5**·2Et₂O, **6**·2MeCN, and **7**·CH₂Cl₂, ESR spectra of **1**, **2**, **4**, **6**, and **7**, ¹H NMR spectra of **4** and **7**, and Chem 3-D drawing of the 3-Me groups superimposed dinuclear bis(μ -hydroxo) complex. This information is available free of charge via the Internet at <http://pubs.acs.org>.

IC9806028